The physics of gamma/neutron spectroscopy

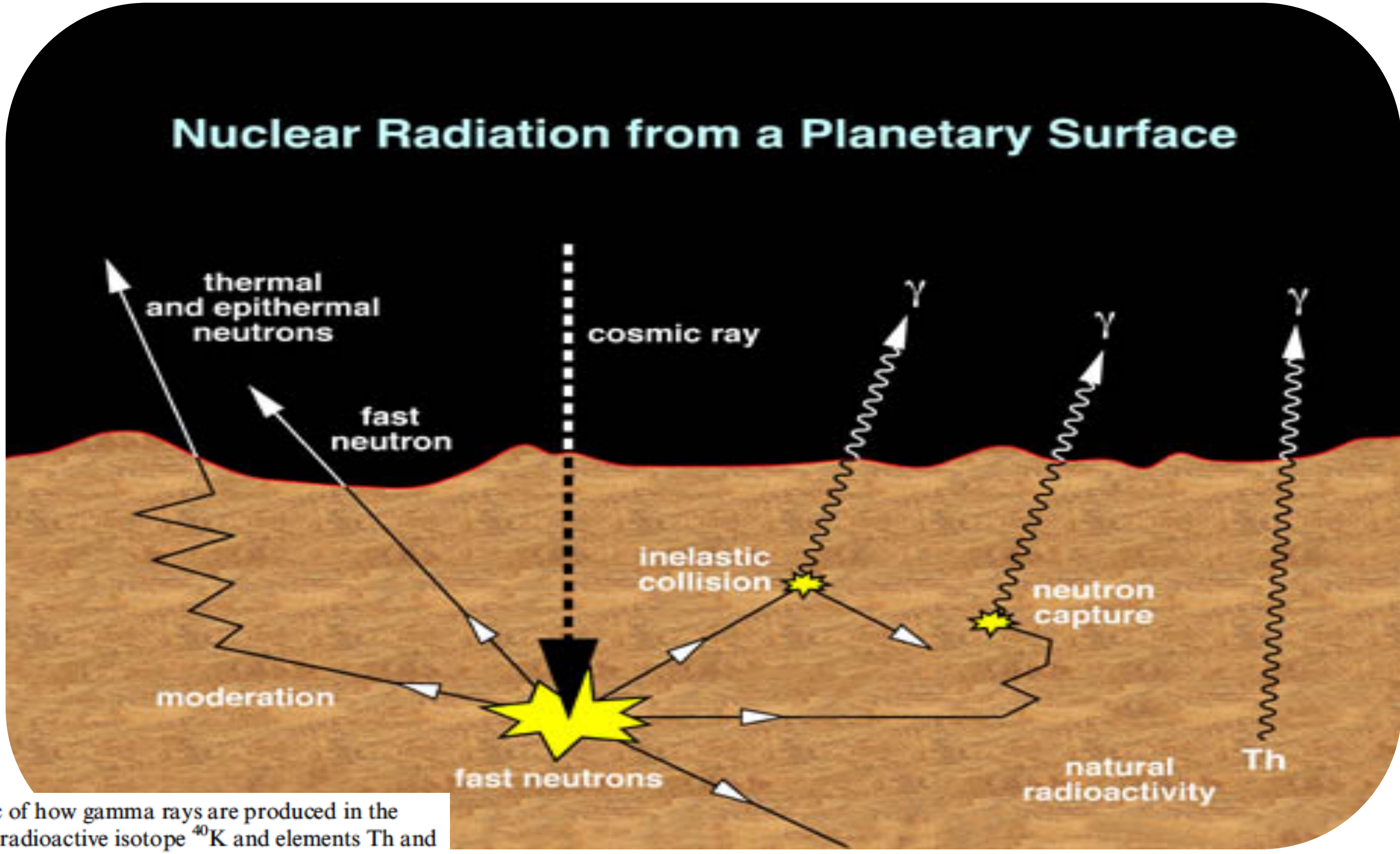

Figure 5.1. Schematic of how gamma rays are produced in the Martian surface. The radioactive isotope ^{40}K and elements Th and U (and their daughter isotopes) produce gamma rays when they decay. The interaction of high-energy (~1–10 GeV) cosmic-ray particles with nuclei in the surface materials produces energetic (fast) neutrons with typical energies of ~1–20 MeV. These fast neutrons can excite elemental nuclei by inelastic-scattering reactions, producing gamma rays. These fast neutrons are moderated by H and other elements, producing slow (thermal, ~0.02 eV) neutrons that can be captured by nuclei and result in the release of gamma rays of specific energies.

Nuclear Remote Sensing

- Background, definitions
- Production mechanisms, elemental sensitivities
- Measurement
- Examples

Background

- Usually used for airless or thin-atmosphered bodies
- Sensitive to elemental/isotopic compositions
- Originate in nuclear transitions

Background (cont'd)

- Energy of photon or particle is most important quantity
  - For gamma rays, energy corresponds to wavelength of photon ($E = h\nu$, or put another way, $E = hc/\lambda$)
  - For neutrons, protons, α particles, etc., energy primarily contained in particle's kinetic energy ($E = mv^2/2$)

- Total Energy is conserved in nuclear interactions

- Typical energies of interest range from "thermal" energies of ~0.02eV up to the 10 GeV (1×10^{10}eV) range

Background (cont'd)

Notation – example reactions:

- ^{16}O absorbs a neutron, ejects a proton, becomes ^{16}N

$$^{16}O(n,p)^{16}N$$

- ^{16}O absorbs a neutron, ejects a lower-energy neutron and a gamma ray, stays ^{16}O. The gamma ray has an energy equal to the difference in energy between the absorbed and ejected neutrons

$$^{16}O(n,n\gamma)^{16}O$$

- ^{16}O absorbs a neutron, ejects an alpha particle and a gamma ray, becomes ^{13}C. Alpha particle has A=4. Since a neutron has A=1, the net change is A=-3.

$$^{16}O(n,\alpha\ \gamma)^{13}C$$

Production of Neutrons and Gamma Rays

- Cosmic rays consist of very high energy protons and other particles from Sun and elsewhere in the galaxy (more on this on the next slide)

- Free neutrons are produced by cosmic ray interactions with the surface

- Gamma rays are produced by neutrons in the surface exciting the nuclei (which then revert to lower energy states by giving up a photon), or by natural radioactive decay

Cosmic Rays

- Cosmic rays are produced by the Sun and by other sources in the galaxy.
- Cosmic rays are composed primarily of very high energy (0.1 – 10 GeV-range) protons (86%), α particles (13%) and other nuclei with $Z>2$ ($<2\%$).
- Cosmic ray flux incident on a planet varies with solar cycles, but averages about 1.5 particles/(cm^2 s)
- Penetration depth in the 10's of g/cm^2. (Note: Earth's atmosphere is about 1000 g/cm^2). Divide by density of surface to get actual depth.

Cosmic rays interact with atmosphere or surface nuclei by *spallation*, which produces fast neutrons in the material (typically ~9 neutrons per cosmic ray particle)

These fast neutrons may:

- Scatter elastically (kinetic energy conserved)
- Scatter non-elastically
  - Inelastic scatter
  - Other non-elastic processes
- Be captured

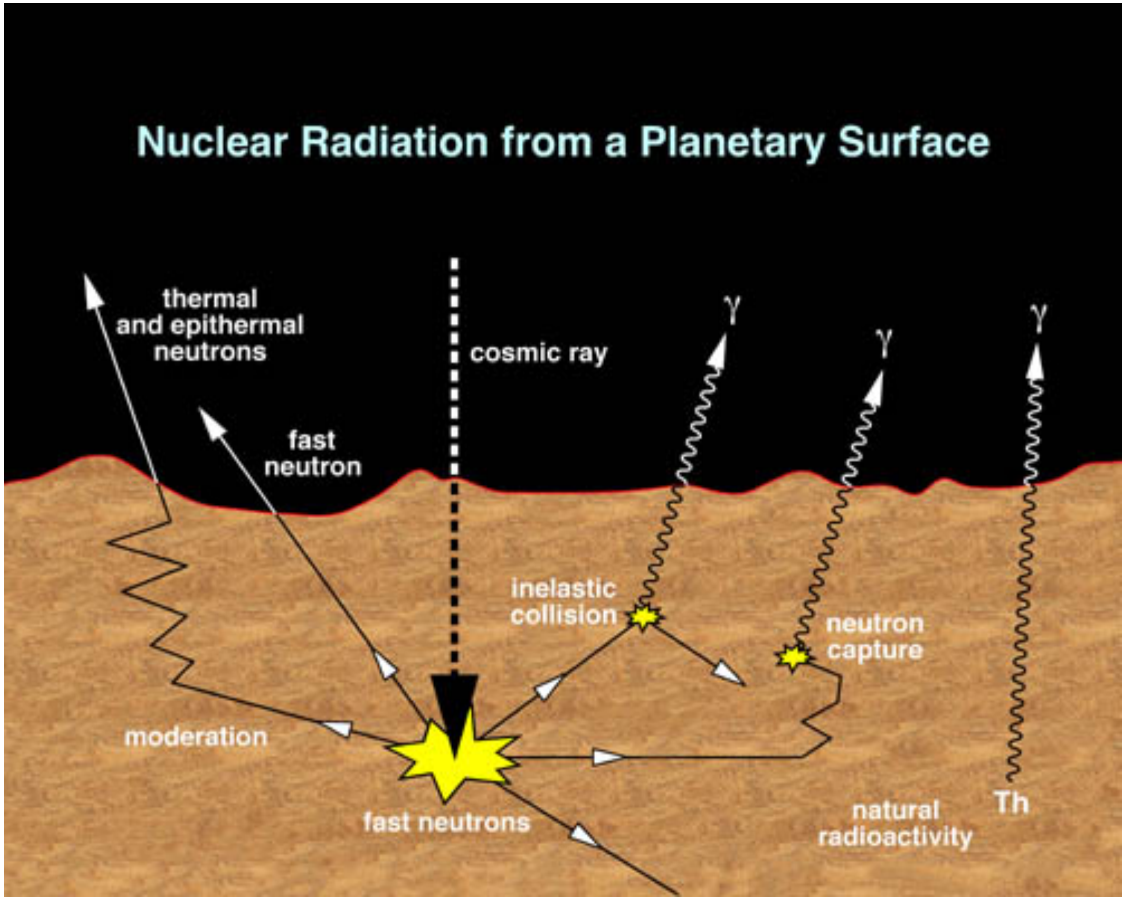

In the end, all neutrons are either captured, or leak out of the surface and eventually undergo beta decay (mean lifetime ~15 min.)

Elastic Scatter

- Neutron collides with nucleus, kinetic energy is conserved. Leaves nucleus unchanged (in ground state) except for recoil.
  - No gamma ray created

Non-Elastic Scatter: Inelastic Scatter

- When neutron collides with nucleus, some kinetic energy is lost. Nucleus is elevated to an excited state. Nucleus then decays back to ground state by releasing a gamma ray.
  - Incident neutron must have higher energy than excited state of nucleus
  - Example: One $^{56}Fe(n,n\gamma)^{56}Fe$ reaction produces a 0.8467 MeV gamma ray

Other Non-Elastic Scattering

- When neutron collides with nucleus, different nucleus is produced
- Can produce gamma ray directly, and/or product nucleus can undergo radioactive decay and produce a gamma ray
- Examples:

$$^{56}\mathrm{Fe}(\mathrm{n},2\mathrm{n}\,\gamma)^{55}\mathrm{Fe}$$

$$^{28}\mathrm{Si}(\mathrm{n},\mathrm{n}\,\alpha\;\gamma)^{24}\mathrm{Mg}$$

Typical elements that produce gamma rays by non-elastic scattering reactions: C, O, Mg, Al, Si, S, Ca, Ti, Fe

Neutron Capture

- Neutron gets added into nucleus, which is elevated to an excited energy state (but not necessarily one of its normal excited levels).
- Usually, nucleus undergoes prompt de-excitation, producing gamma rays.
- Sometimes produces a longer-lived radioactive nucleus, which subsequently decays and produces gamma rays

Typical elements that produce gamma rays by neutron capture:

H, Al, Si, Cl, Ca, Ti, Cr, Fe, Ni

Gamma Ray Spectra from a Surface

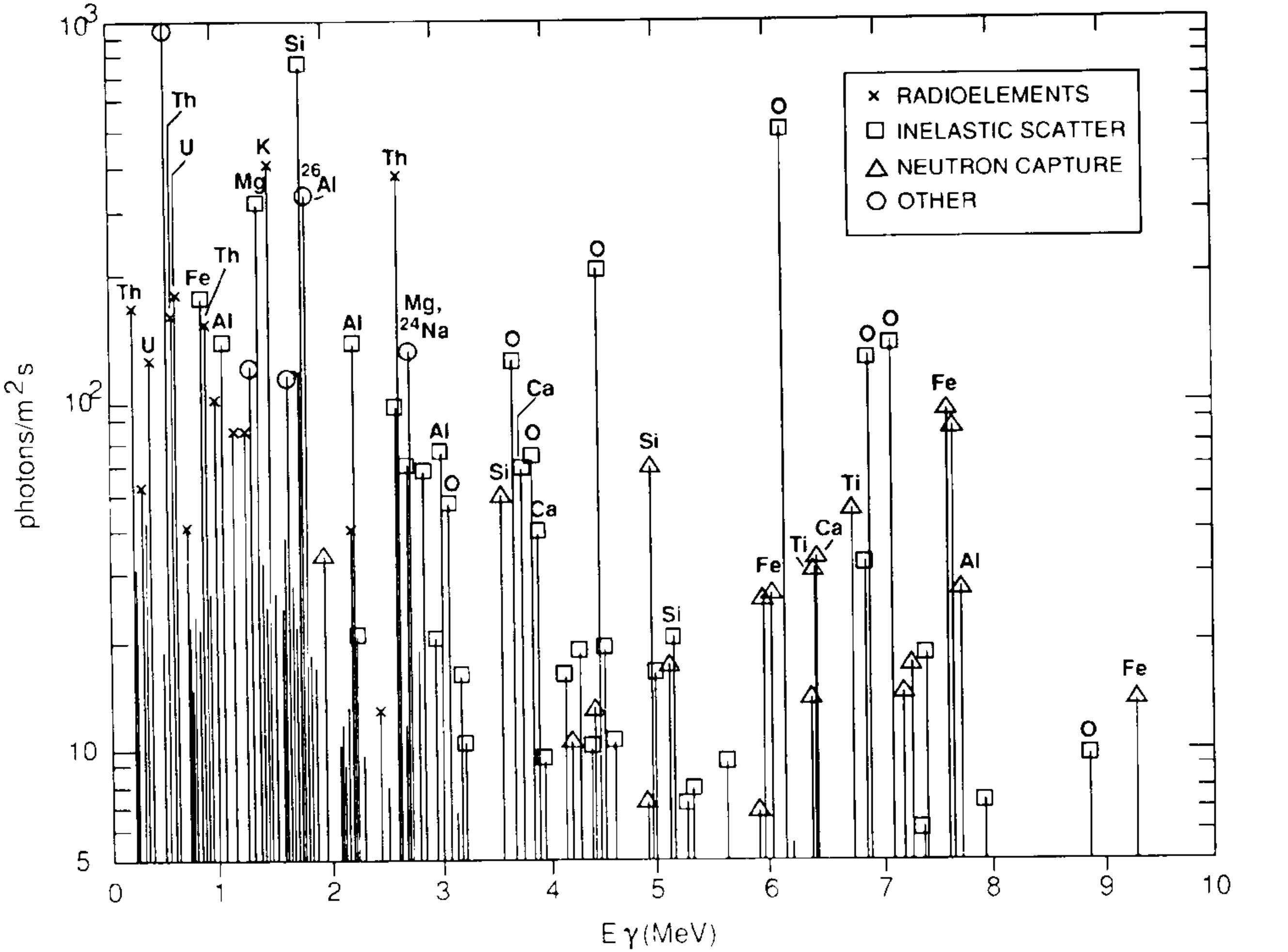

Example: Gamma Rays emerging from the lunar surface

Gamma spectroscopy: element sensitivity

depends on abundance, radioactivity, atmosphere & instrument components (e.g., Mg)

TABLE III

Calculated accumulation times required to achieve 10% percision.

Element	Energy (keV)	Mode	Model Composition	Signal (c/s)	Continuum (c/s)	Time for 10% precision (hr)
H	2223	Capture	0.11%	0.0017	0.24	2400
O	6129	Inelastic	42.3%	0.0223	0.34	20
Mg	1369	Inelastic	5.2%	0.0124	0.37	70
Al	2210	Inelastic	4.2%	0.0029	0.24	820
Al	7724	Capture	4.2%	0.0008	0.25	12000
Si	1779	Inelastic	19.8%	0.0468	0.29	4
Si	3539	Capture	19.8%	0.0035	0.15	370
S	5424	Capture	2.7%	0.0021	0.37	2200
Cl	6111	Capture	0.55%	0.0081	0.34	150
K	1461	Radioactive	0.51%	0.1074	0.35	1
Ca	1943	Capture	4.7%	0.0018	0.27	2300
Mn	7244	Capture	0.4%	0.0009	0.28	9100
Fe	847	Inelastic	17.3%	0.0268	0.59	24
Fe	7632	Capture	17.3%	0.0130	0.26	44
Th	2614	Radioactive	0.30 ppm	0.0037	0.20	430
U	1765	Radioactive	0.078 ppm	0.0011	0.30	6800

Boynton et al. (2004)

Gamma ray spectra

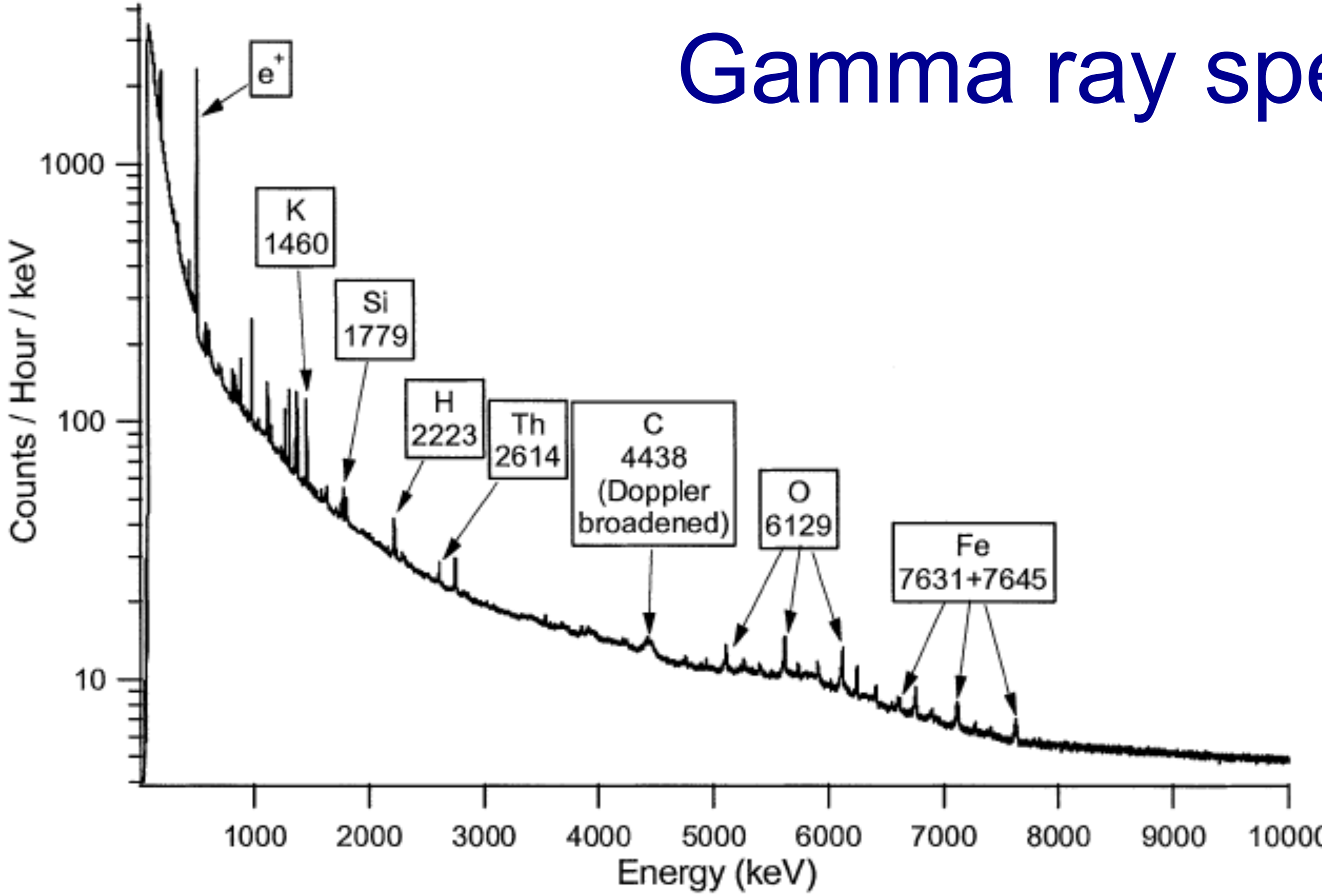

Figure 8. A GS spectrum of Mars taken from June 10 through July 16, 2002. Several emission lines are labeled with their energy in keV and the element responsible for the line. This shows our full-scale energy range of 10 MeV at our nominal gain setting. The continuum above about 8 MeV is due mostly to charged particle interactions in the detector. The broad continuum at lower energies is due mostly to scattered gamma rays that have lost a fraction of their energy. Scattering can occur in the regolith, the atmosphere, or the instrument itself. The line labeled e^+ is due to one of the two 511-keV gamma rays that occur when positrons and electrons annihilate. Positrons are made in one of the processes by which high-energy gamma-rays can interact with matter. The high-energy lines in the spectrum occur in threes, with the lines separated by 511 keV. The lower-energy lines are due to the loss of one or both of the 511 keV gamma rays made when a high-energy photon interacts with the detector via the pair production process.

Boynton et al. (2004)

Gamma ray spectra

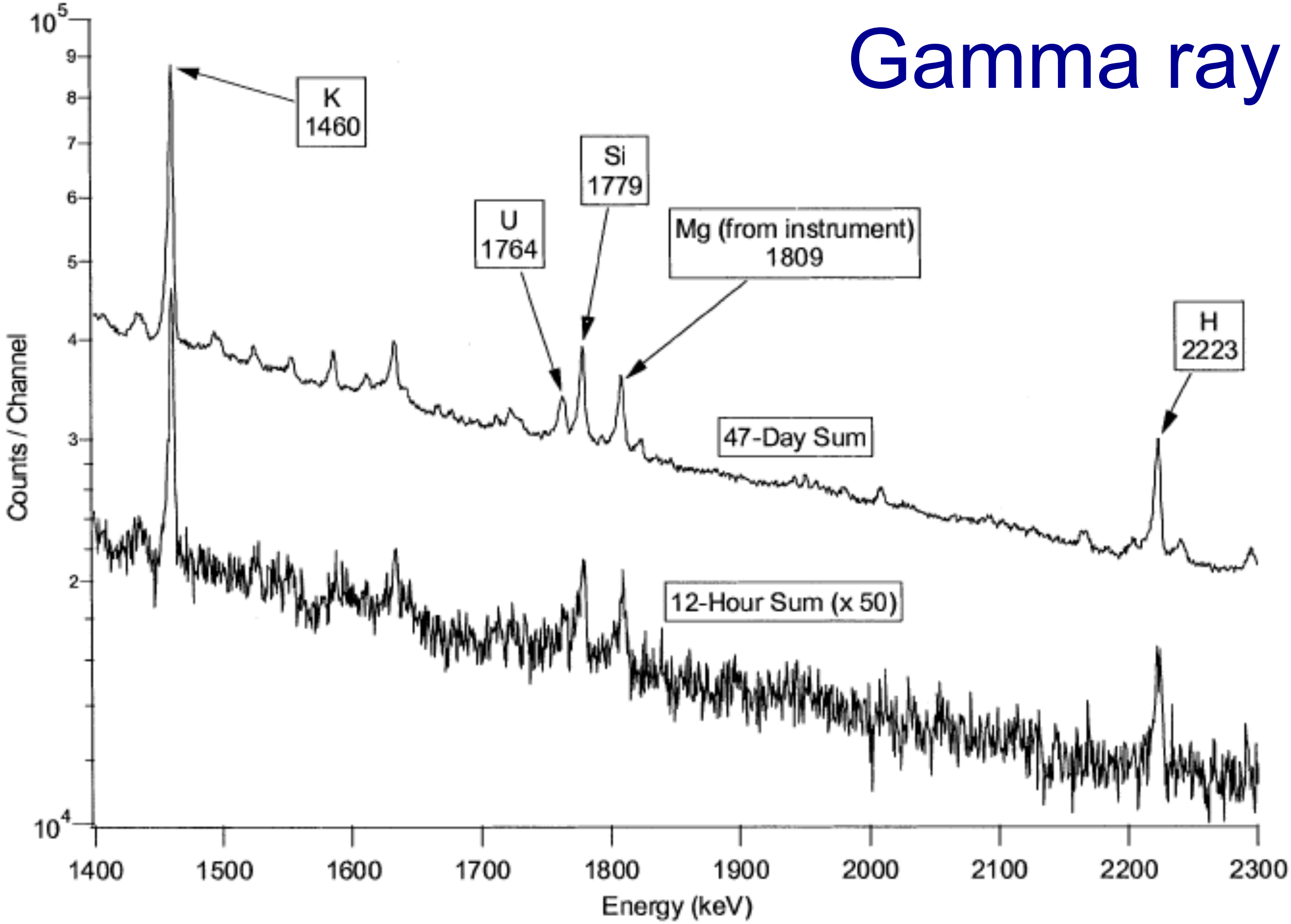

Figure 9. An expanded portion of the full-Mars GS spectrum shown in Figure 8 with a similar spectrum but with a much shorter accumulation time. The nature of the peak shapes can be seen; the area of the peak above the continuum is proportional to the concentration of the element responsible for the gamma-ray emission. The short-duration spectrum, collected for 12 hours, is what is expected for a 450-km footprint at middle latitudes. The uranium line is barely detectable in this spectrum, which shows the importance of being able to sum spectra together over larger regions to improve statistics for weak peaks.

Boynton et al. (2004)

Orbital gamma mapping: ***low*** spatial resolution

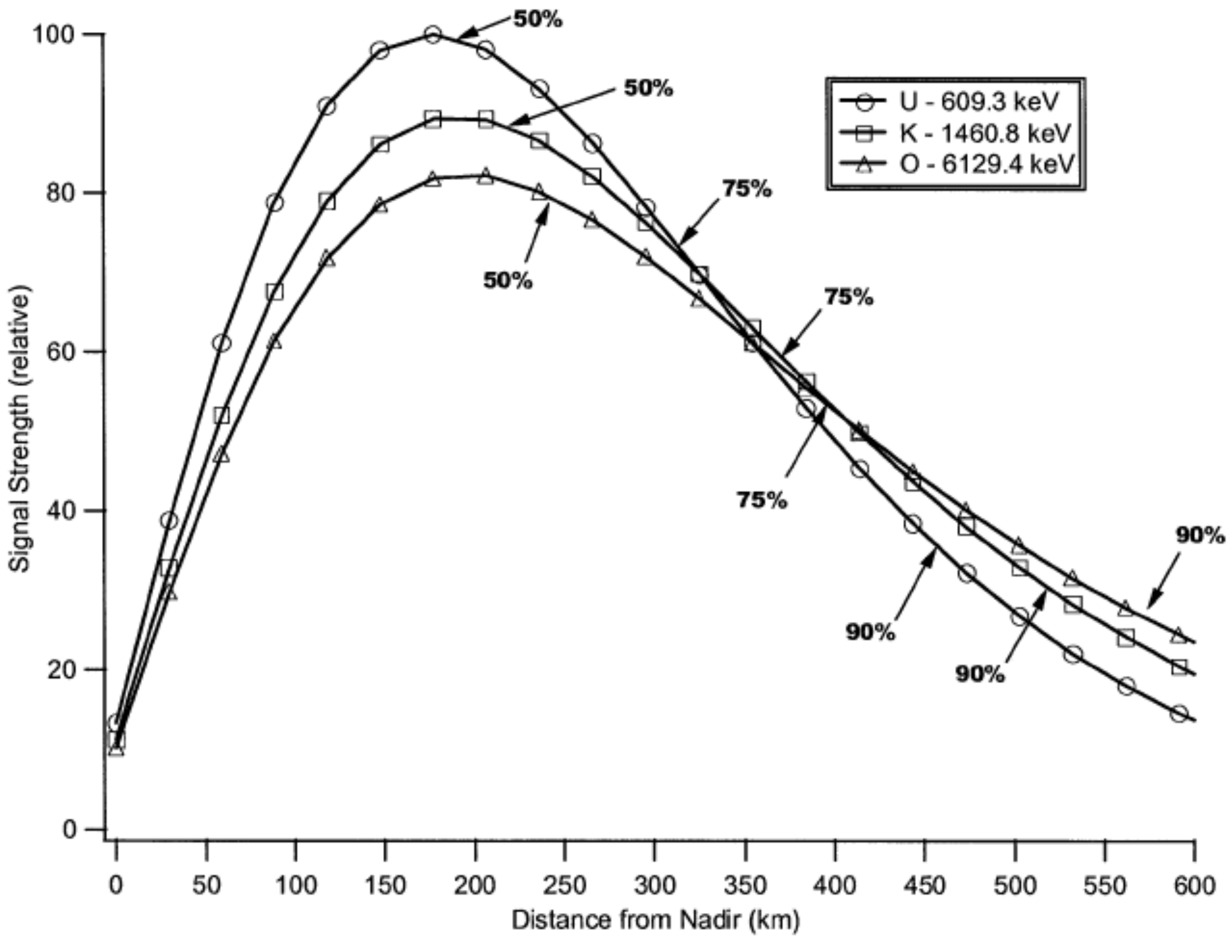

Figure 1. Signal intensity as a function of distance from the sub-spacecraft point (nadir) for three different gamma-ray energies. The signal increases with distance from nadir because the area of each annulus gets bigger, but it then drops off due to attenuation through greater path length through the regolith and atmosphere. The distance is indicated inside of which 50% of the signal is collected. This diagram is generated for a nominal Mars atmospheric thickness of 15 g/cm^2. At low elevations on Mars, where there is a thicker atmosphere, the spot size is smaller, and at higher elevations it is greater.

Boynton et al. (2004)

The Ones That Got Away: Neutron Leakage Spectra

- Some neutrons are able to exit the surface before being captured
- The energies of these neutrons depends on their scattering history
  - Fast neutrons that scatter in surfaces with a substantial abundance of low-mass nuclei (comparable in mass to the neutron) lose their energy ("moderate") to these nuclei in successive scattering events
  - Fast neutrons that have mostly scattered off high-mass (more massive than the neutron) nuclei lose much less of their energy

Nuclear Radiation from a Planetary Surface

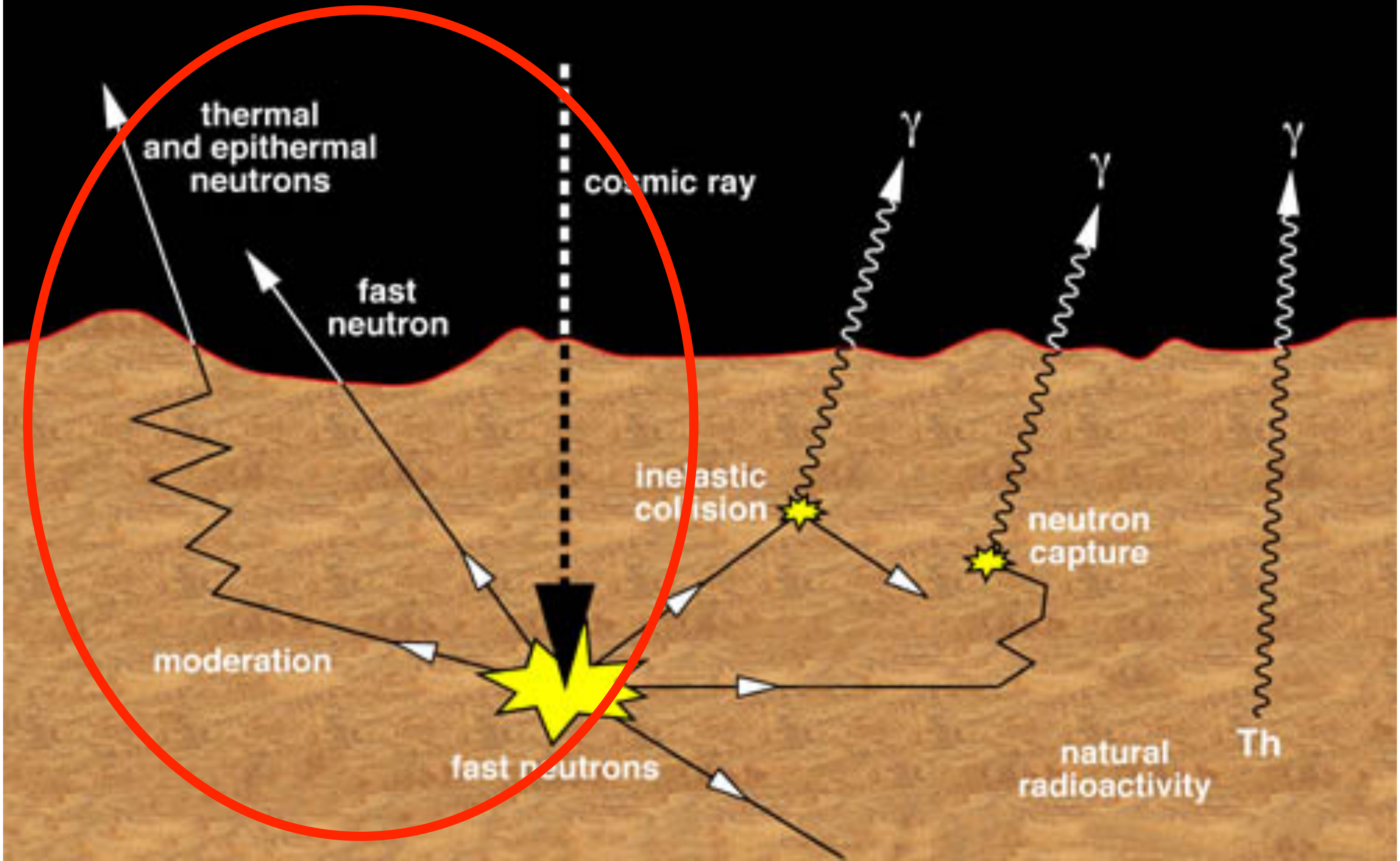

Neutron detection of H

By far the most efficient moderator of fast neutrons is H because the next lightest nucleus is 4x heavier.

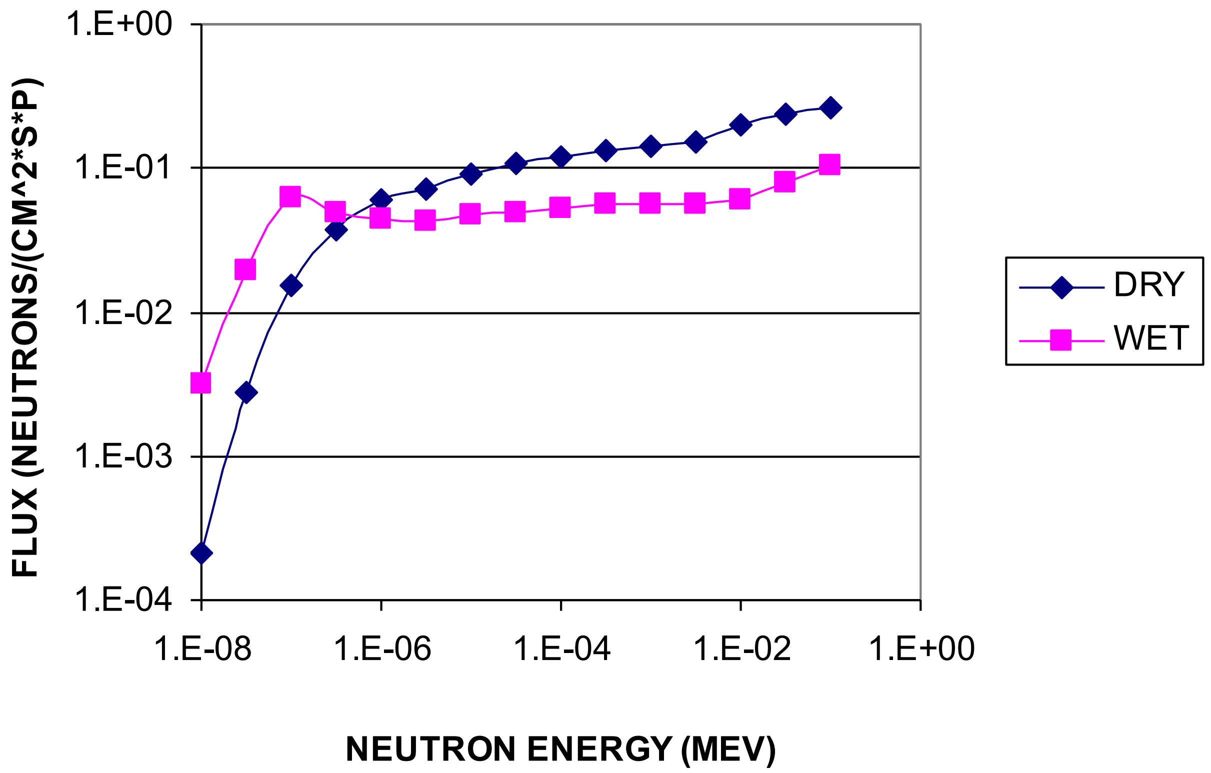

Detection and Mapping of Gamma Rays and Neutrons

- Two types of gamma ray detectors:
  - Scintillation detectors: Gamma ray excites electrons, which de-excite by emitting visible wavelength photons (scintillation). The number of photons produced is proportional to the energy deposited by the gamma ray. Relatively poor energy resolution.
  - Solid state detectors: Gamma ray excites electrons, which produces electron-hole pair (like in a semiconductor). A field applied to the crystal sweeps the charge to an electrical pulse detector. Good energy resolution, but crystal becomes damaged over time – must anneal periodically.

Detector Complications

Three ways a gamma ray can interact with solid state detector:

- Photoelectric absorption: Gamma ray energy is completely absorbed in the detector (desirable).
- Compton scattering: Gamma ray only partially loses energy through interactions with electrons. Can produce a range of energies less than the original gamma ray energy (undesirable).
- Pair production: Gamma ray interaction with detector produces an electron-positron pair. Pair subsequently annihilates, producing two 0.511 MeV gammas. None, one, or both of these can leak out of detector. Total energy deposited is initial gamma energy, initial gamma energy minus 0.511 MeV, or initial gamma energy minus 2 x 0.511 MeV (gives three lines).

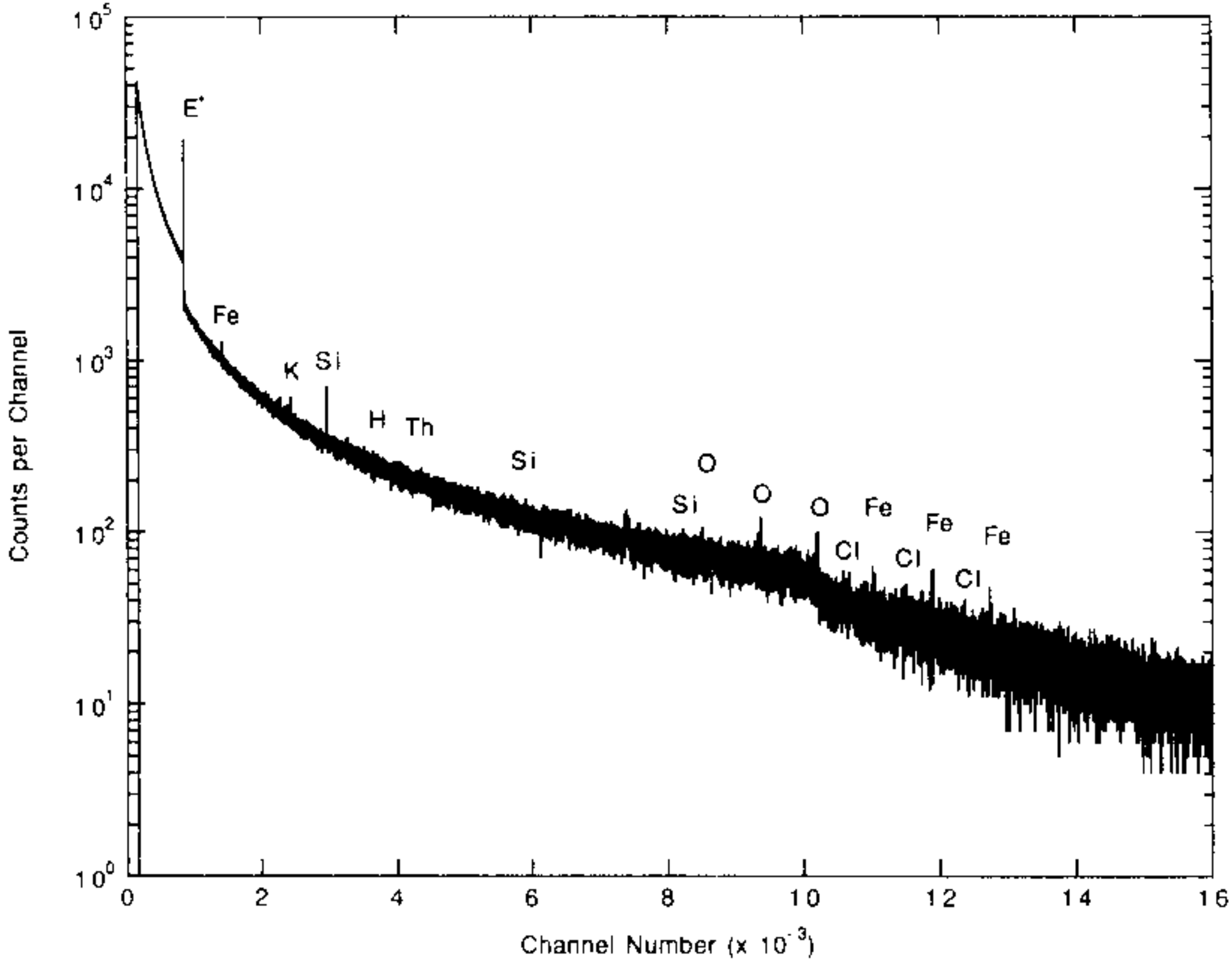

E*
Fe
K
Si
H
Th
Si
O
Si
O
O
Fe
Cl
Fe
Cl
Fe
Cl
10^5
10^4
10^3
10^2
10^1
10^0
Counts per Channel
0
2
4
6
8
10
12
14
16
Channel Number (x 10^-3)

Neutron Detection

- As part of a gamma ray instrument: Some gamma ray instruments cannot tell difference between energy deposited by gamma ray vs. particles. Many use an "anti-coincidence" shield around the detector that is sensitive only to particles, not photons. Can act as a neutron detector.
- As a stand-alone: Neutrons may also be detected by themselves. Example is ^{3}He tube detector. With two tubes – one bare, the other wrapped in Cd – one can distinguish fast neutrons from slow ones.

Mapping Considerations

- All detectors discussed are "4 π steradian detectors" (they see gamma rays or particles from all directions) – can't point them.
  - For an orbiter-based platform, instrument sees all the way to the local horizon. The ground footprint has a diameter comparable to the orbital altitude.

- Gamma rays and neutrons are counted one at a time. Derivation of abundances depends on the statistical significance of the number counted at a particular energy (proportional to square root of number of counts).
  - Getting good statistics on weak gamma ray lines from particular elements can take many, many orbits

Mapping of natural terrestrial radioisotopes

Airborne gamma-ray spectrometry surveys can assist exploration for many commodities, most obviously for U and Th, but commonly also for Sn, W, REE, Nb and Zr.

Less often, but of importance in specific circumstances, radiometric anomalies can point to Au, Ag, Hg, Co, Ni, Bi, Cu, Mo, Pb, and Zn mineralization, either because one or more of the radioelements is an associated trace constituent or because the mineralizing process has changed the radioelement ratios in the surrounding environment.

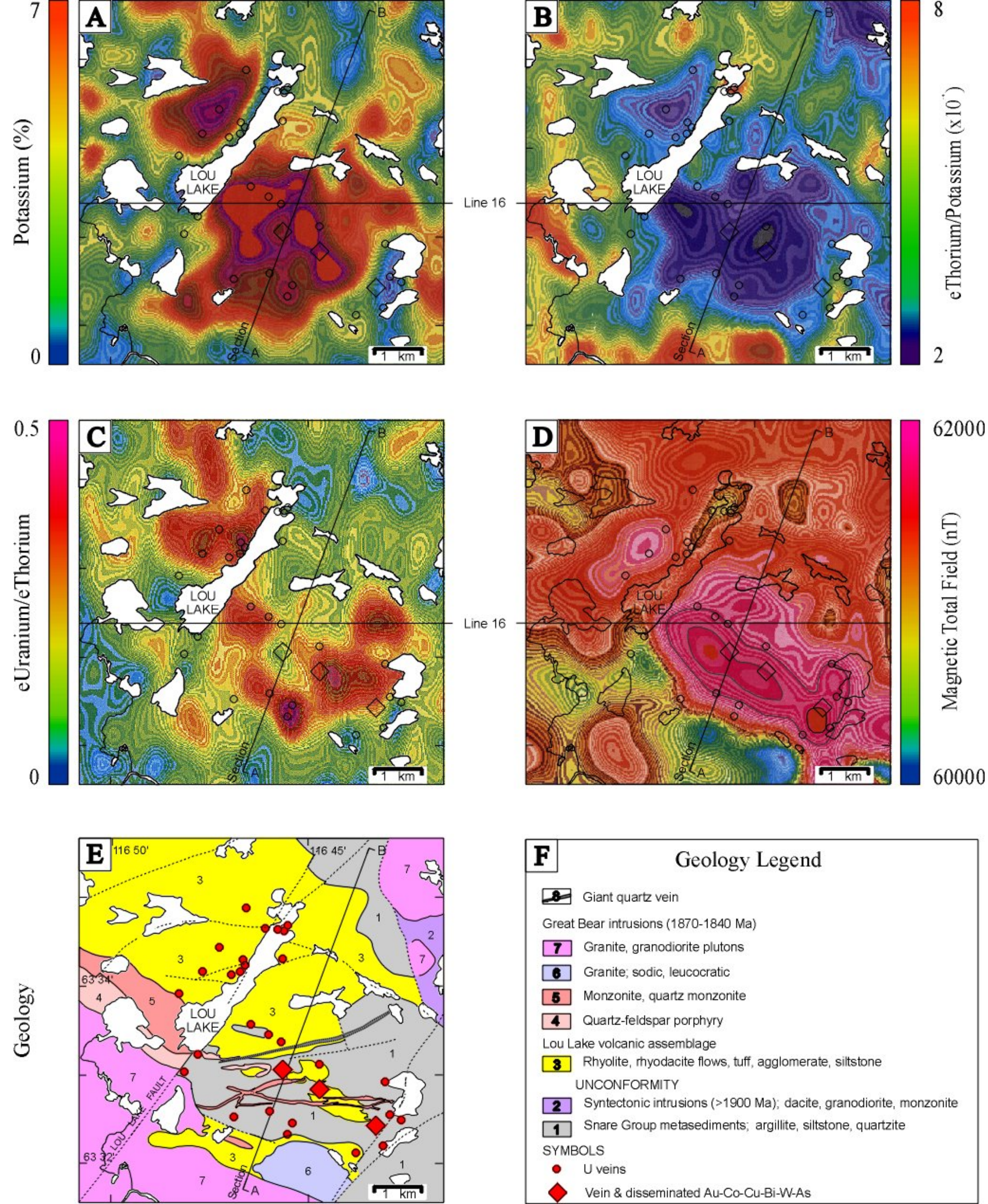

Major Elements

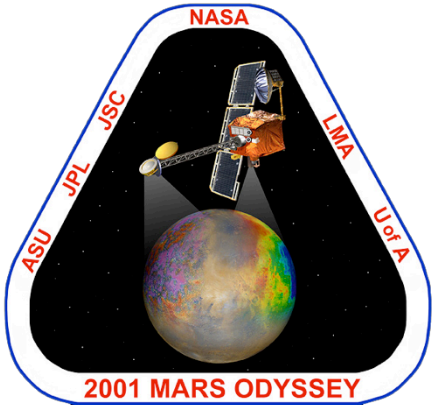

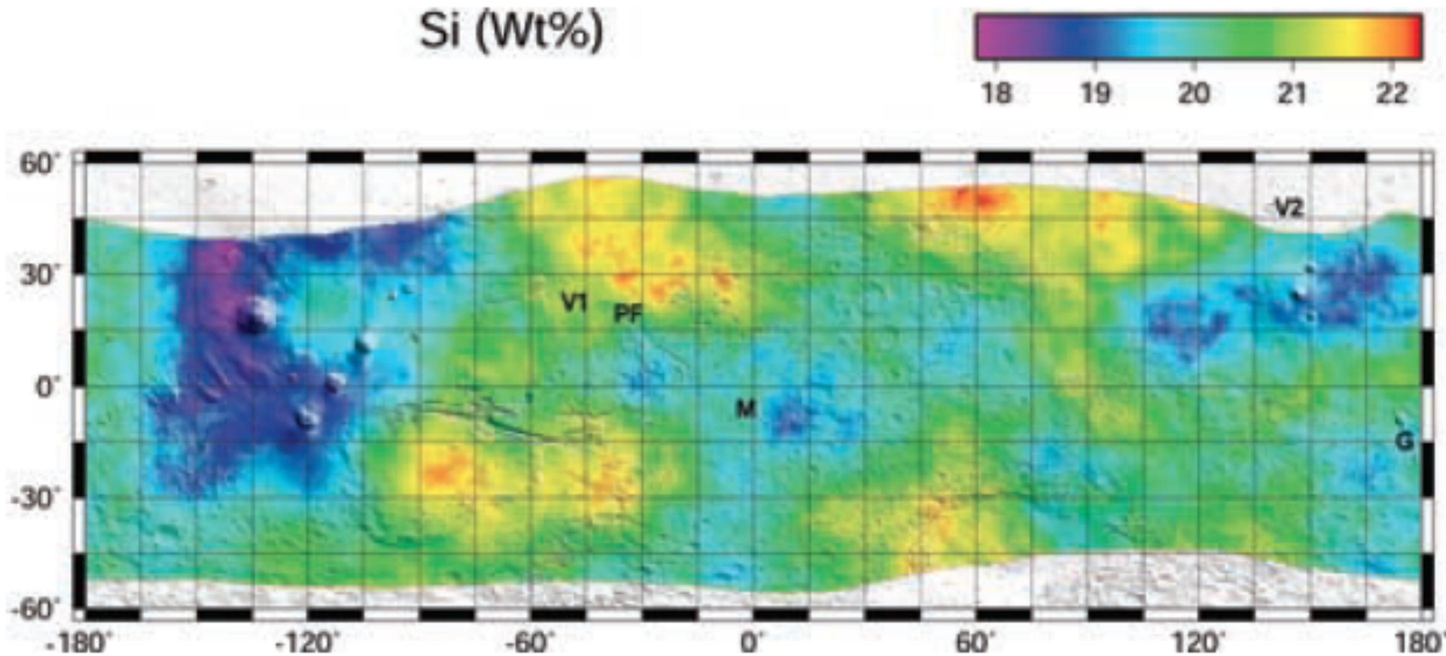

Also have fairly good maps of Ca, Al

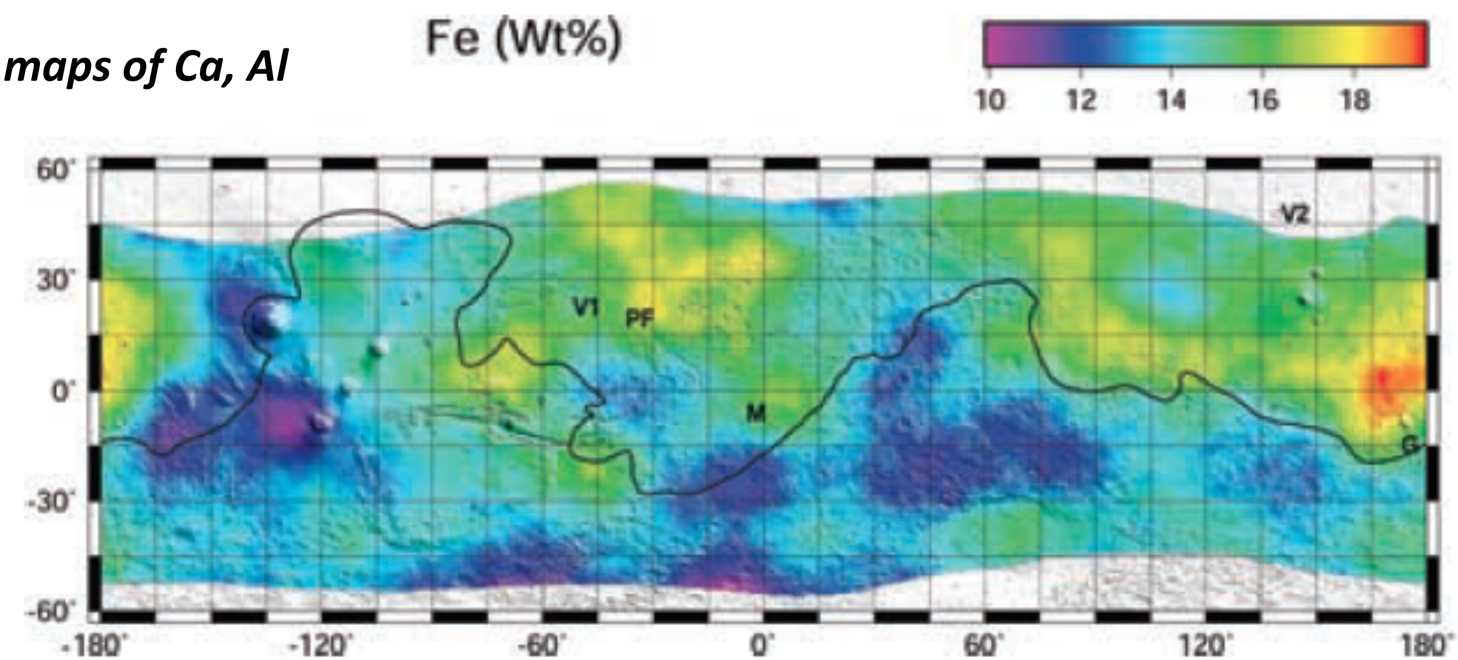

Boynton et al. (2007)

Volatile Elements

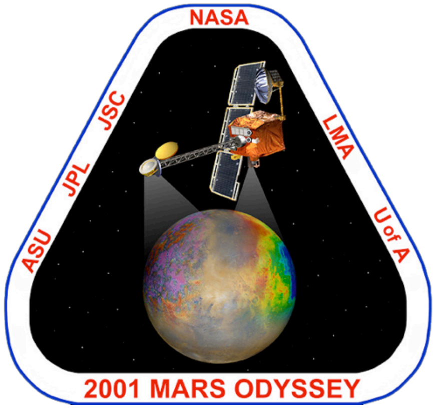

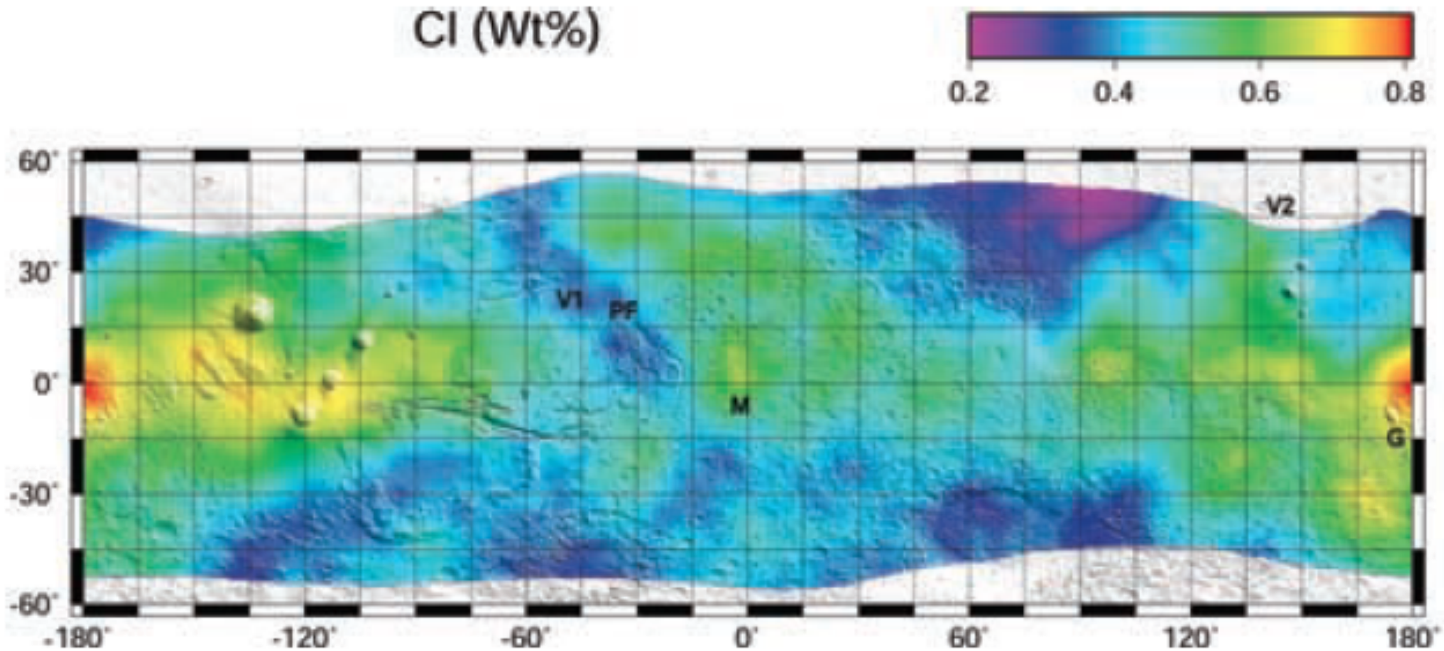

Have a fairly good S map now too

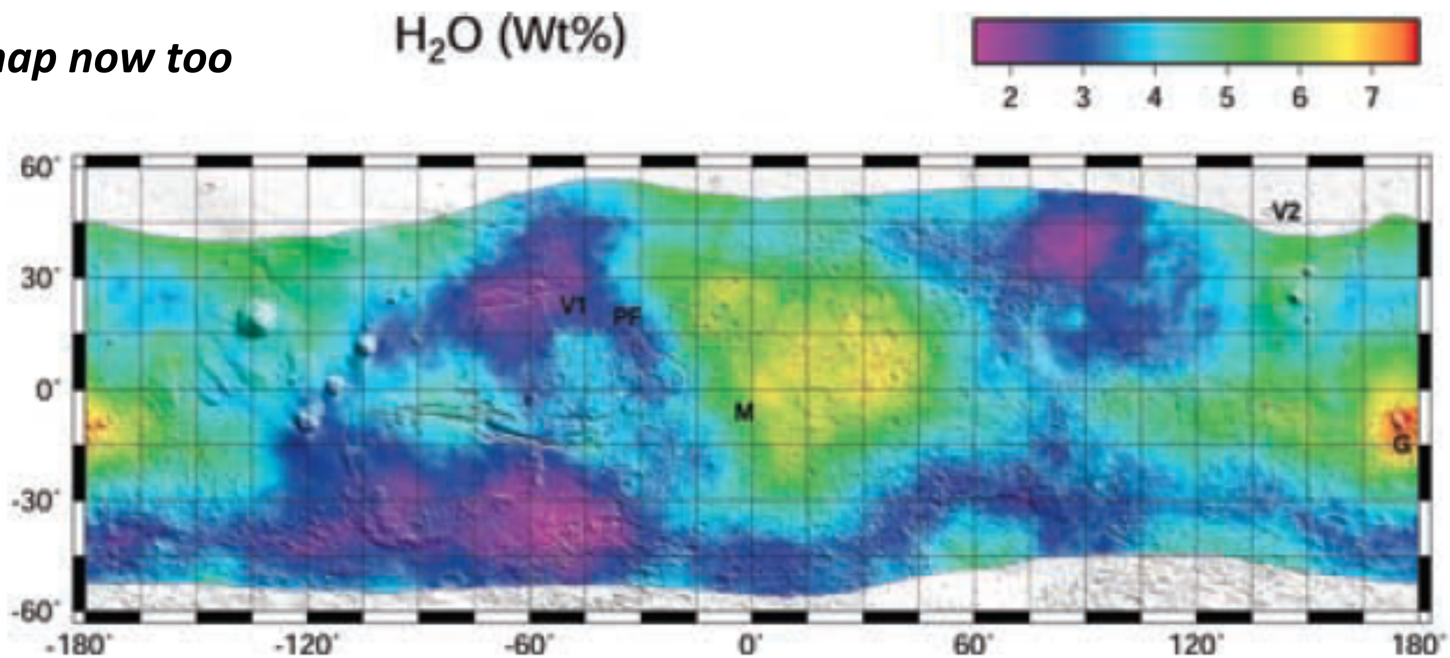

Boynton et al. (2007)

Radioactive Elements

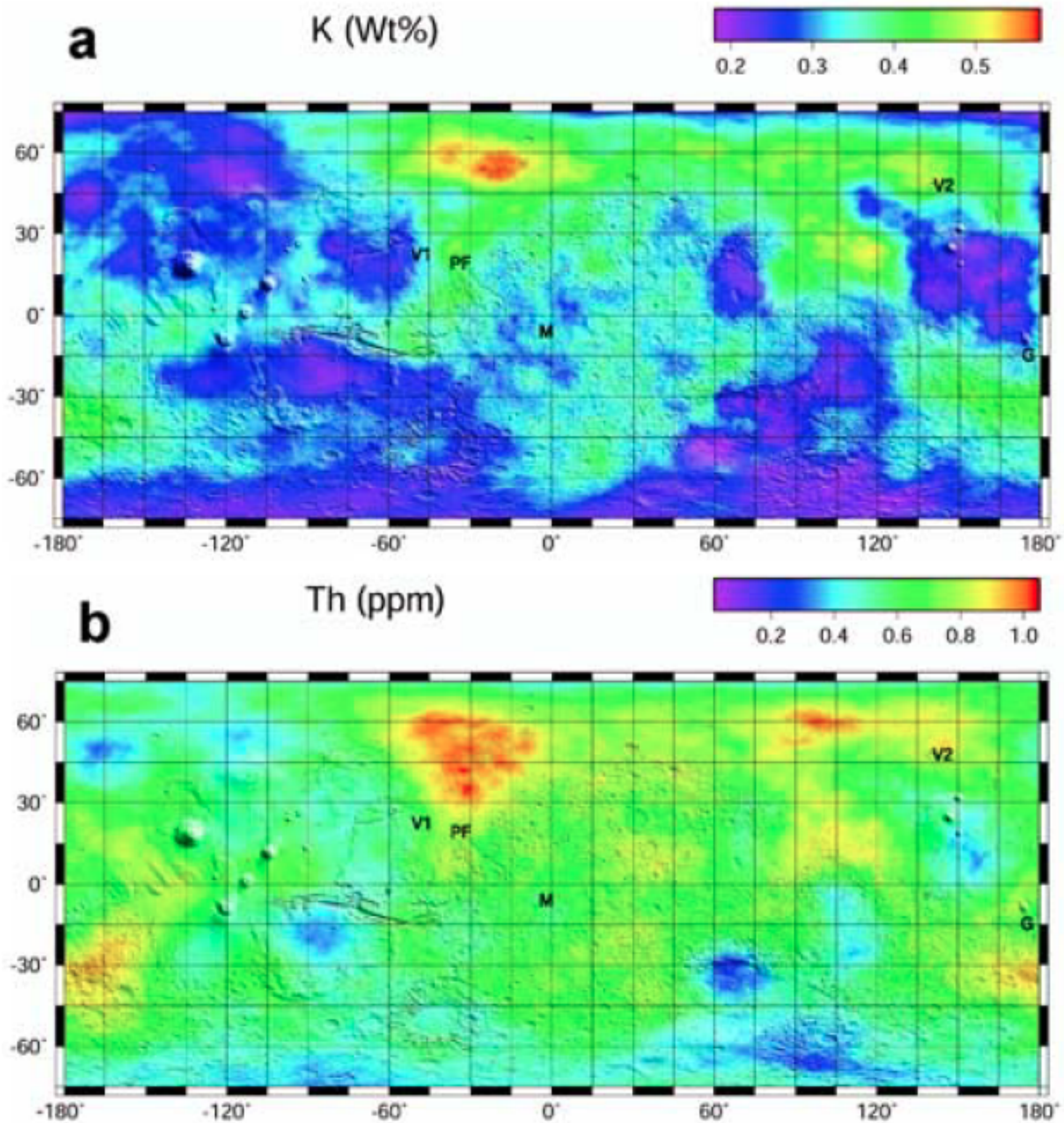

Boynton et al. (2007)

Get most insight from regions with ***correlated elemental anomalies***

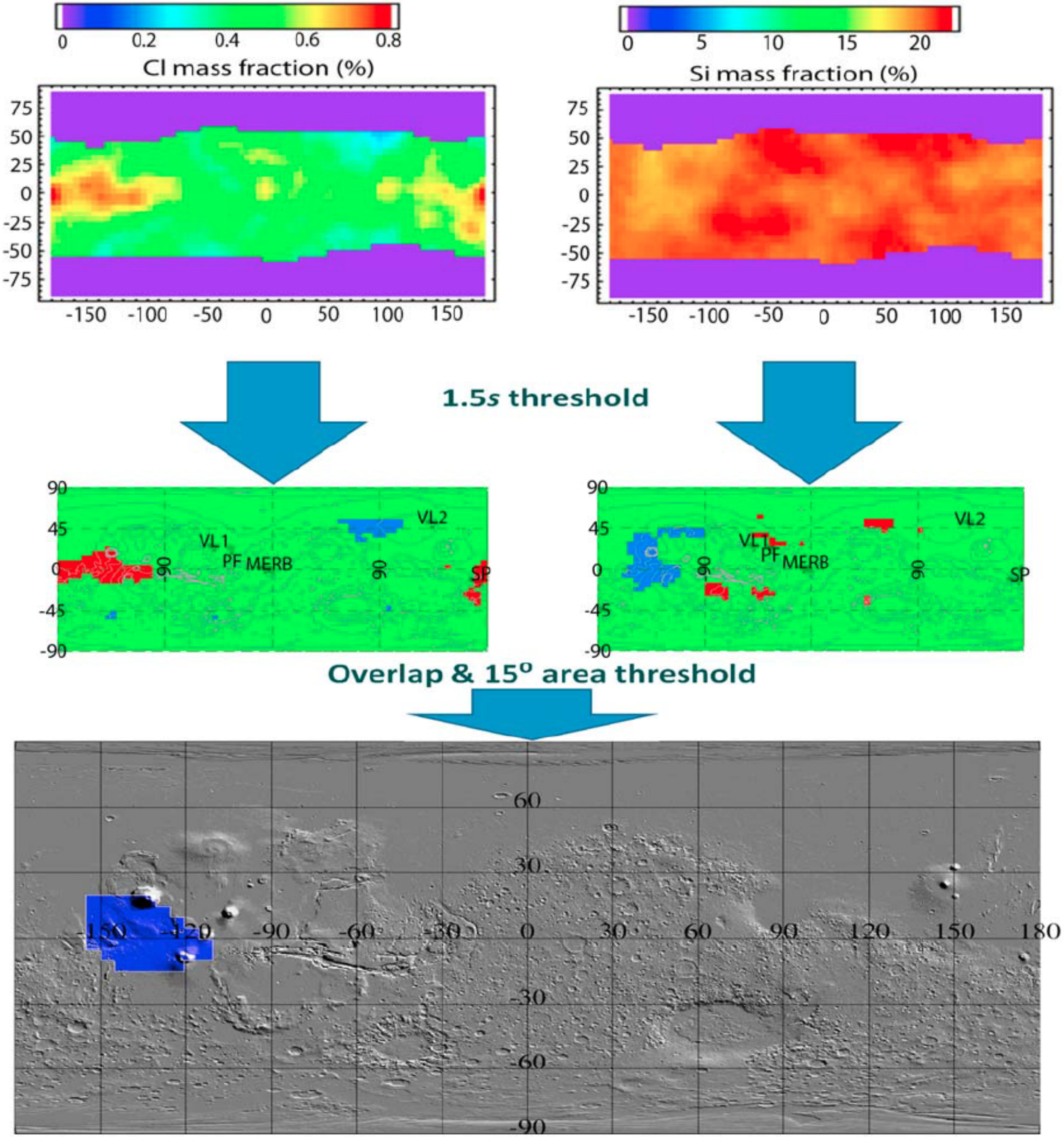

Karunatillake et al. (2009)

"Chemically striking regions" defined by correlated elemental anomalies

Table 3. Key to the Numerical Code of Chemically Striking Regions in Figure 3[a]

Key	Value
Unclassified	0
{Al, Fe} 1s ED 15°	5
{Cl, H} 1s EE 15°	10
{Cl, H} 1s EE 15° {Cl, Si} 1s ED 15°	15
{Cl, Si} 1.5s ED 15°	20
{Cl, Si} 1s DE 15°	25
{Cl, Si} 1s DE 15° {K, Th} 1s EE 15°	30
{Cl, Si} 1s ED 15°	35
{Fe, Th} 1s EE 15°	40
{Fe, Th} 1s EE 15° {K, Th} 1.5s EE 10°	45
{Fe, Th} 1s EE 15° {K, Th} 1.5s EE 10° {Si, Th} 1s EE 15°	50
{Fe, Th} 1s EE 15° {K, Th} 1s EE 15°	55
{Fe, Th} 1s EE 15° {K, Th} 1s EE 15° {Si, Th} 1s EE 15°	60
{Fe, Th} 1s EE 15° {Si, Th} 1s EE 15°	65
{H, Si} 1s DE 15°	70
{H, Si} 1s DE 15° {K, Th} 1s DD 10°	75
{K, Th} 1.5s EE 10°	80
{K, Th} 1.5s EE 10° {Si, Th} 1s EE 15°	85
{K, Th} 1s DD 10°	90
{K, Th} 1s DD 15°	95
{K, Th} 1s EE 15°	100

[a]Each chemically striking region (CSR) is denoted by the corresponding set of elements in curly braces, confidence (Table 2) as an approximation to a multiple of the standard deviation (*s*), enrichment (E) and/or depletion (D) in element order, and arc radius of the area threshold (Table 1). For example, {Cl, Si} 1.5s ED 15° would denote a bin belonging to a single CSR marked by the enrichment of Cl and depletion of Si at better than 1.5*s* confidence and exceeding a 15° radius area. On the other hand, {Cl, H} 1s EE 15° {Cl, Si} 1s ED 15° identifies a bin of overlap between two CSRs: One {Cl, H} 1s EE 15° and the other {Cl, Si} 1s ED 15°. Note that such bins generally do not delineate a sufficiently large contiguous area to be classified as a CSR in its own right. CSRs of Si and Th overlap completely with the CSRs of K and Th albeit at different statistical confidence levels. The one region on the basis of Al is solely to motivate future investigations as the Al map is being refined. Higher numerical uncertainties and weak correlation with other elements caused the absence of Ca-based CSRs.

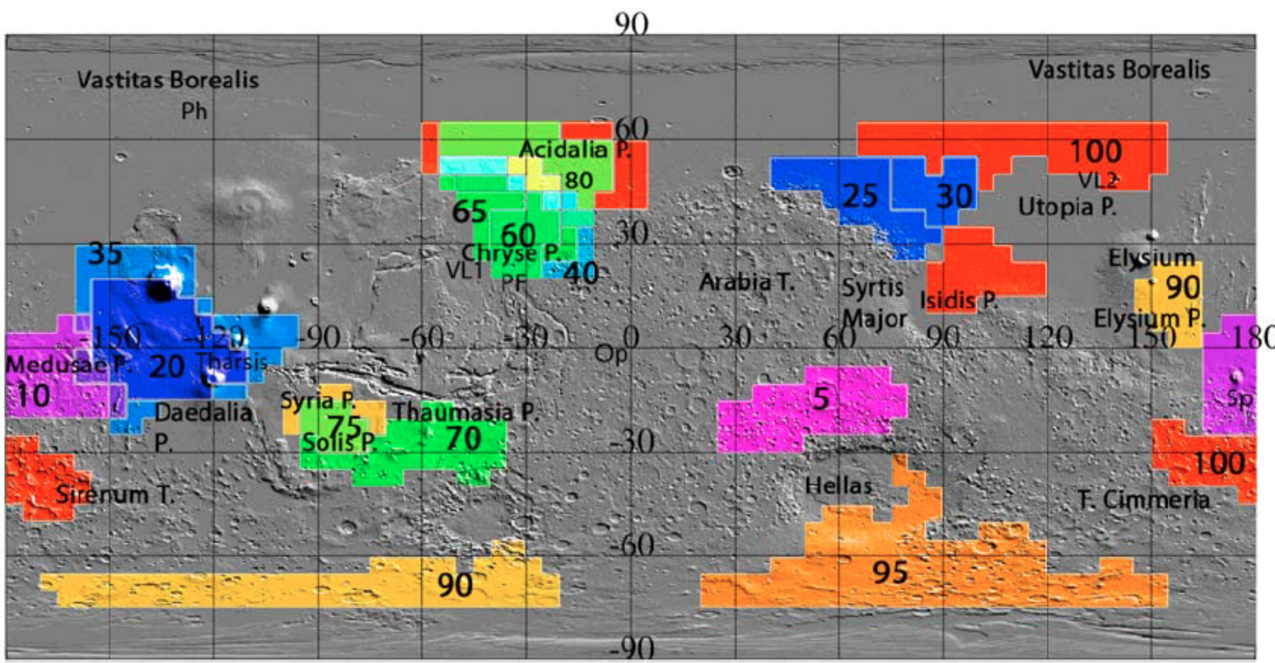

Karunatillake et al. (2009)

"RAVE" – a Cl-rich, Si/Fe-poor region

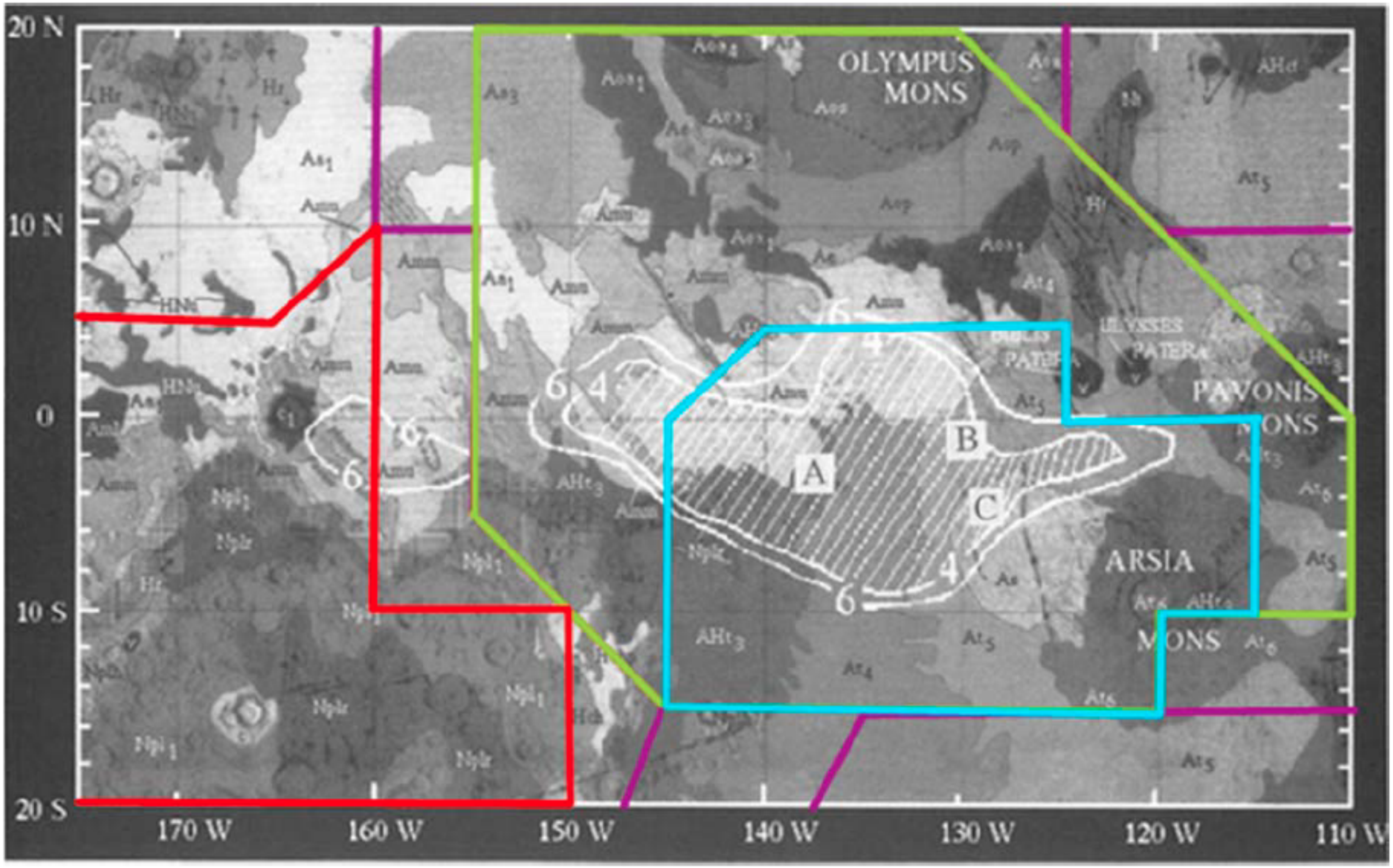

Figure 11. Sketch of RAVE (sky blue) overlain on Stealth region at 3.5 cm and mapped geologic units (adapted from *Edgett et al.* [1997, Figure 4]). Note the striking spatial overlap between RAVE and Stealth of greatest confidence (hatched region) relative to the Medusae Fossae formation units: Amm, Amu, and Aml. The surrounding CSRs include {ClSi ED 1.5s 15°} in lime and {ClSi ED 1s 15°} in purple. Surficial chemical differences between eastern and western Medusae Fossae are revealed by {ClH EE 1s 15°} CSR (red) to the west and {ClSi ED 1s 15°} to the east.

Karunatillake et al. (2009)

“RAVE”: brightness, low thermal inertia → dust

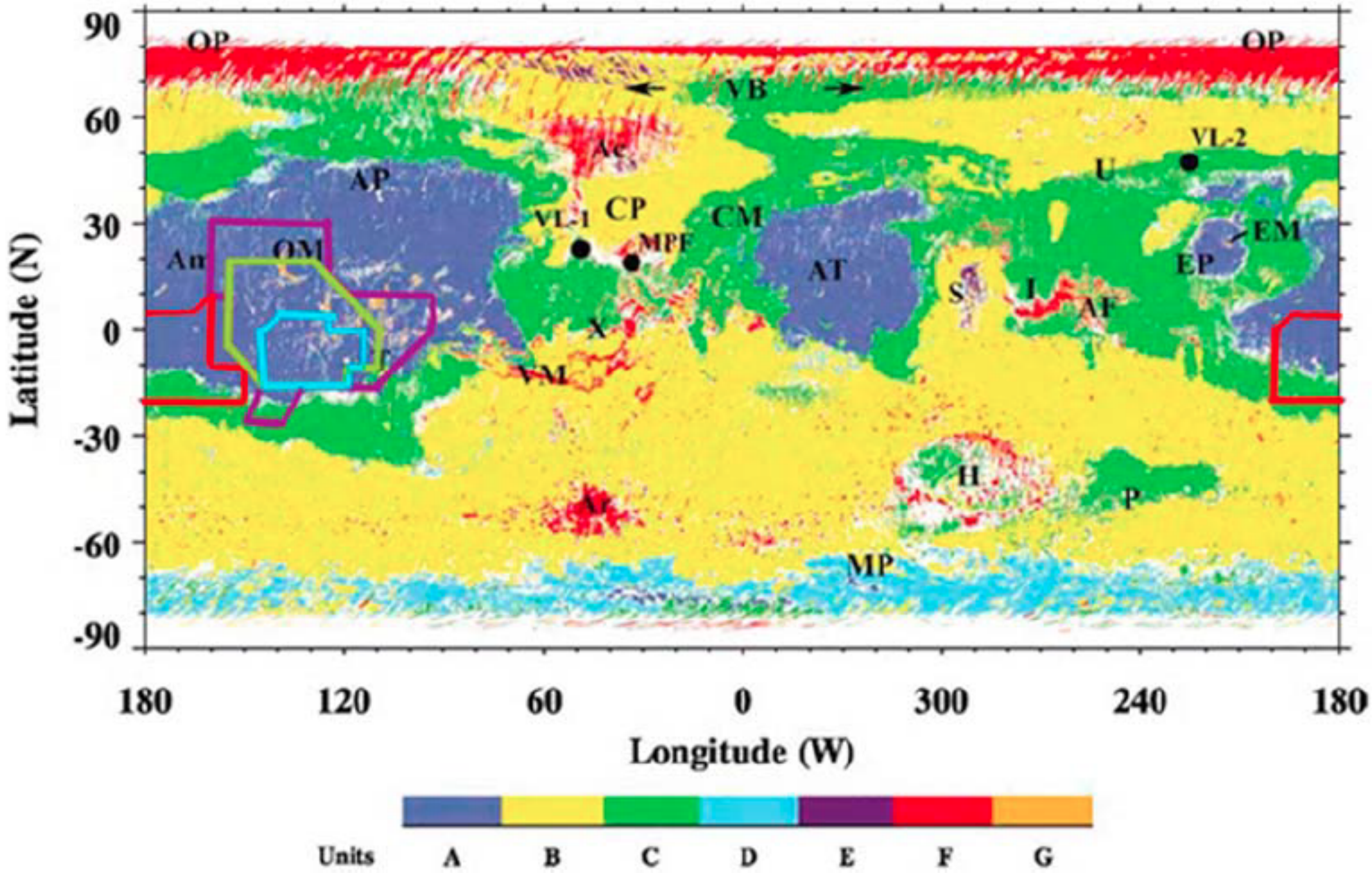

Figure 12. Sketch of RAVE (sky blue line) overlaid on the thermal inertia/albedo unit map (adapted from *Putzig et al.* [2005, Figure 5] with permission from Elsevier). RAVE is contained entirely within the low thermal inertia/high-albedo unit (blue) as is the bulk of the two surrounding CSRs. These are {ClSi ED 1.5s 15°} outlined in lime and {ClSi ED 1s 15°} outlined purple. The {ClH EE 1s 15°} to the west is outlined red and its southern portion is filled in green indicating high thermal inertia and medium albedo.

Karunatillake et al. (2009)

"RAVE": high-resolution imagery → blanketed by dust

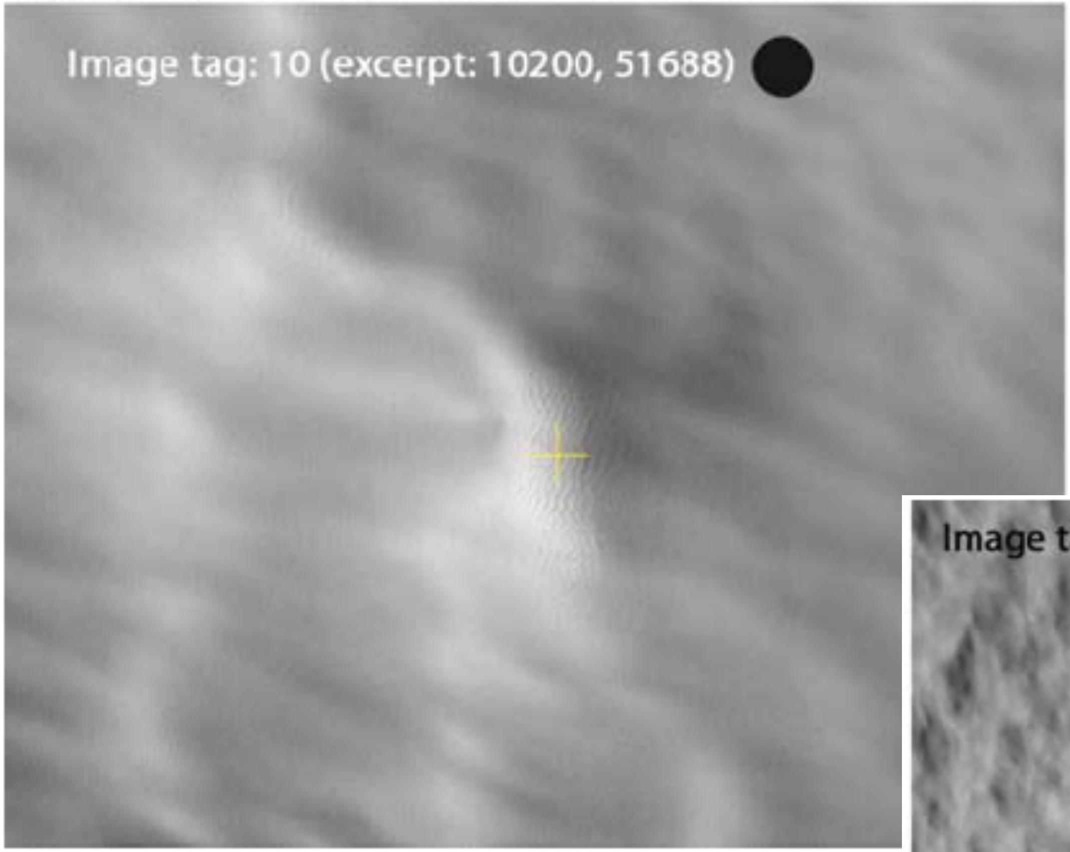

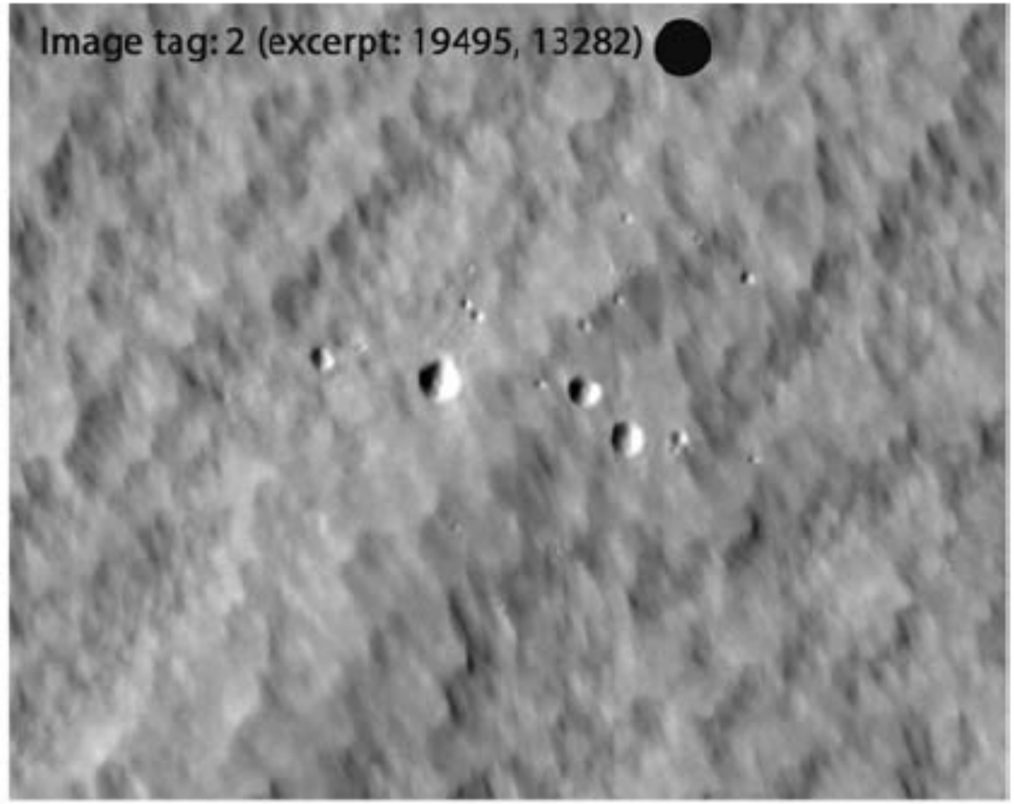

Black circles are 10 meters across

Karunatillake et al. (2009)

Chemical comparisons: RAVE similar to dust at rover sites, but with less Si and more Ca

→ ***dust diluted & cemented by Ca-salts??***

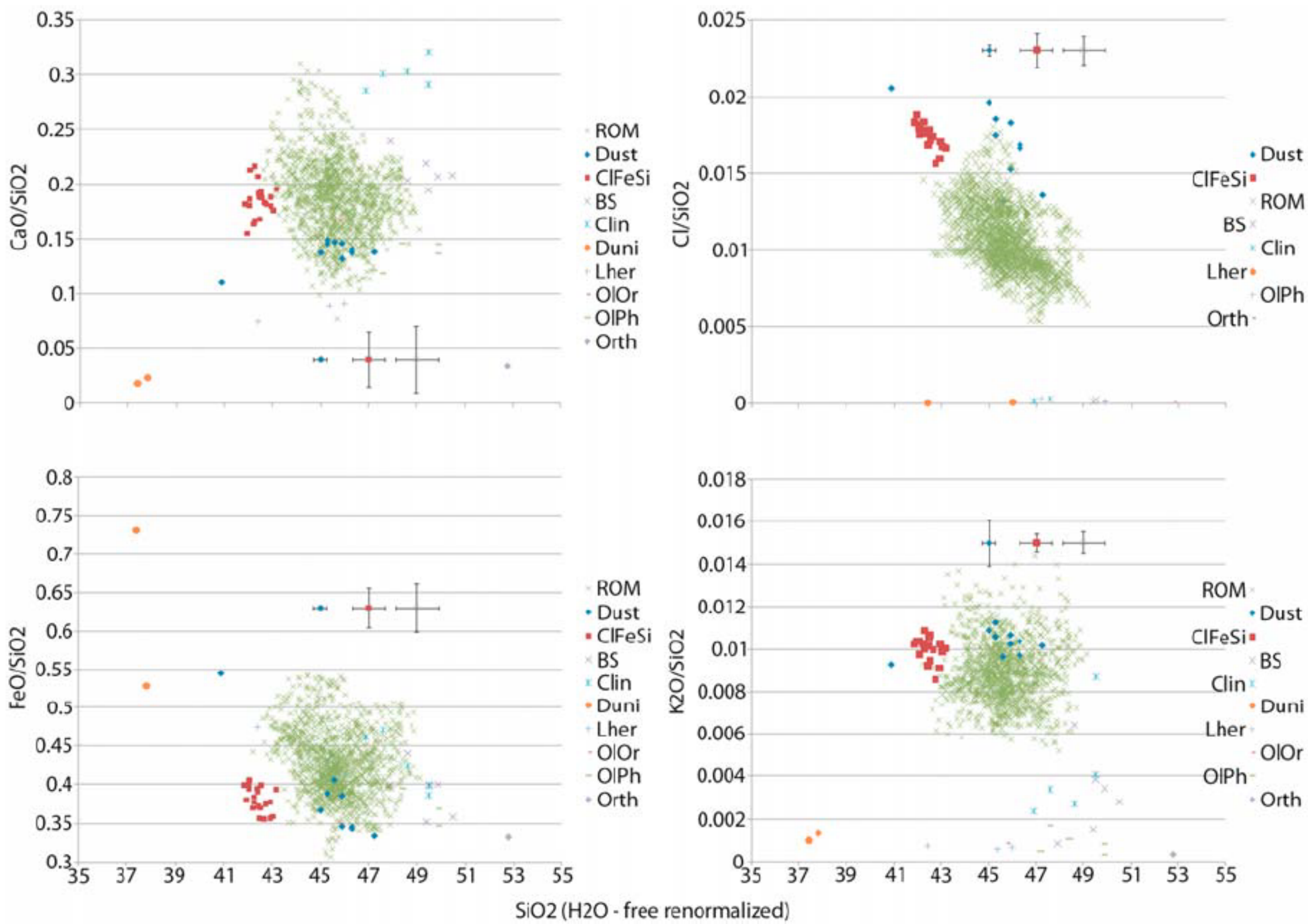

Figure 24. Scatterplots of oxide mass fraction to SiO_2 mass fraction ratios versus the SiO_2 mass fraction for SNC meteorite classes and RAVE (legend, ClFeSi) with the rest of Mars (ROM) and dust included

Karunatillake et al. (2009)

Apollo Gamma-ray Spectrometer Iron Abundance

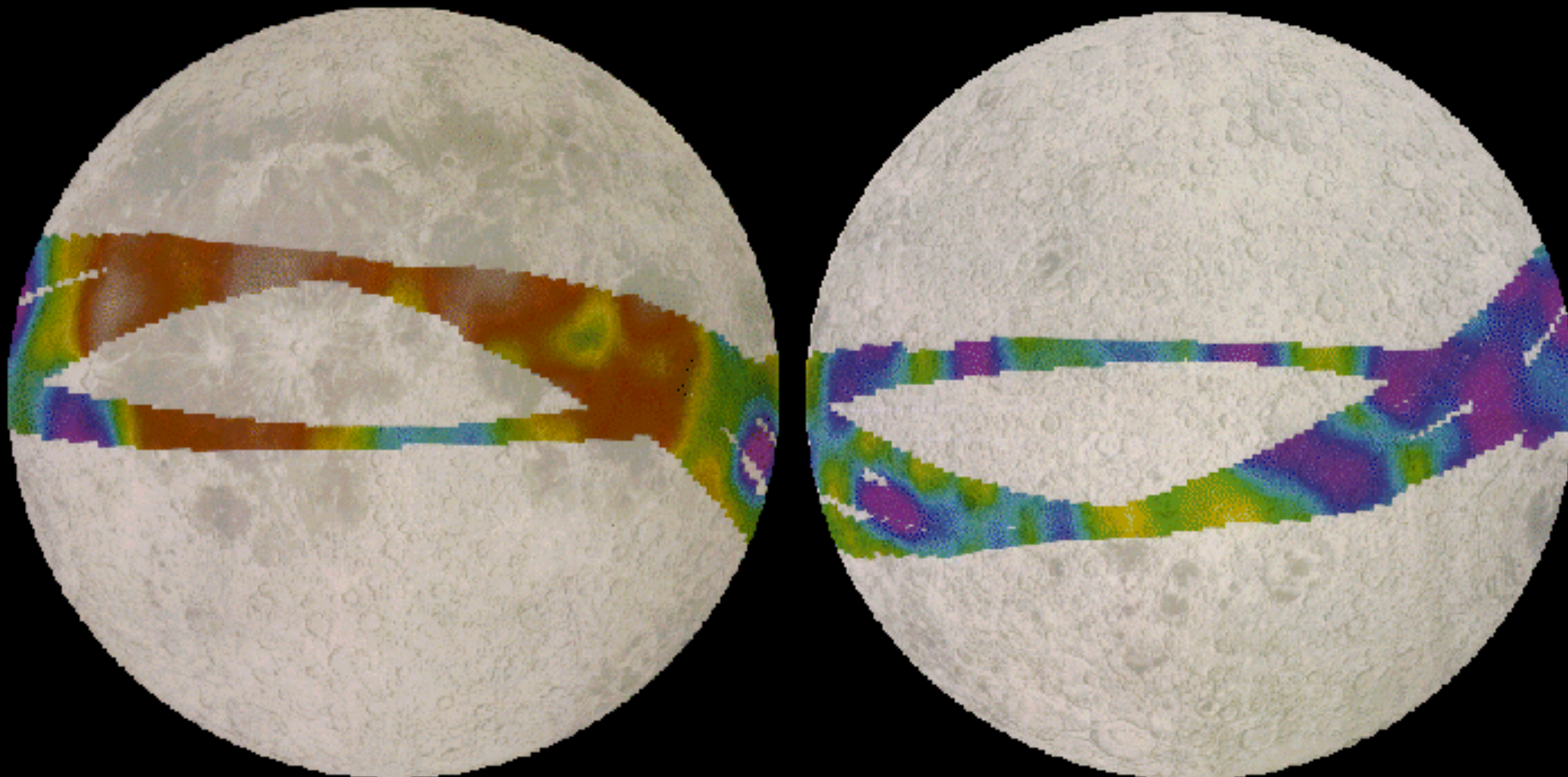

Nearside

Farside

Lunar KREEP (potassium, rare-Earth elements, phosphorus)

- From Moon's middle layer, between anorthositic highlands and olivine/pyroxene-rich mantle
- In samples from every Apollo site … but all Imbrium basin ejecta?

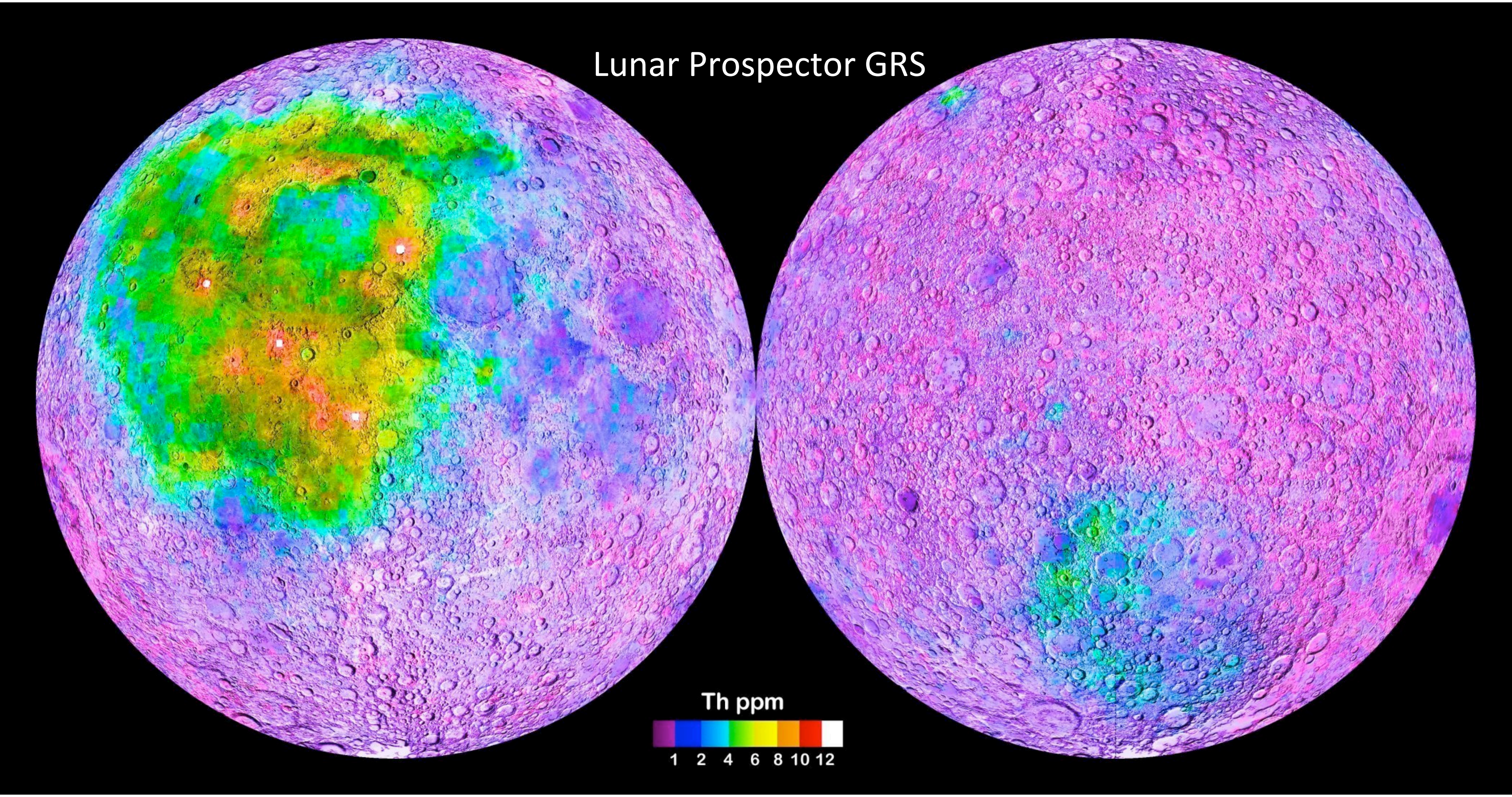

For a great explanation, see: http://www.planetary.org/blogs/emily-lakdawalla/2011/3013.html

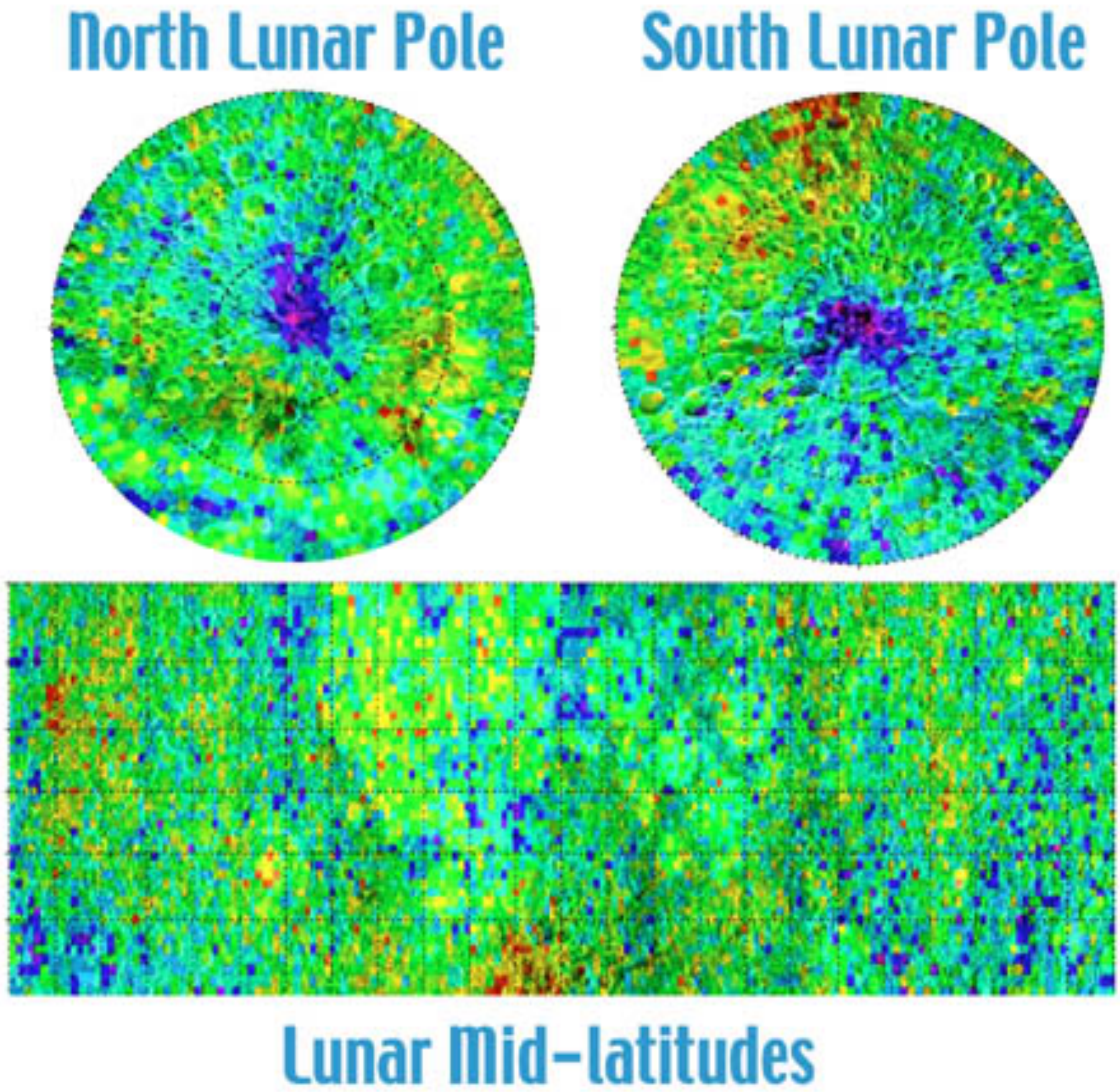

Lunar hydrogen map from Lunar Prospector neutron detector

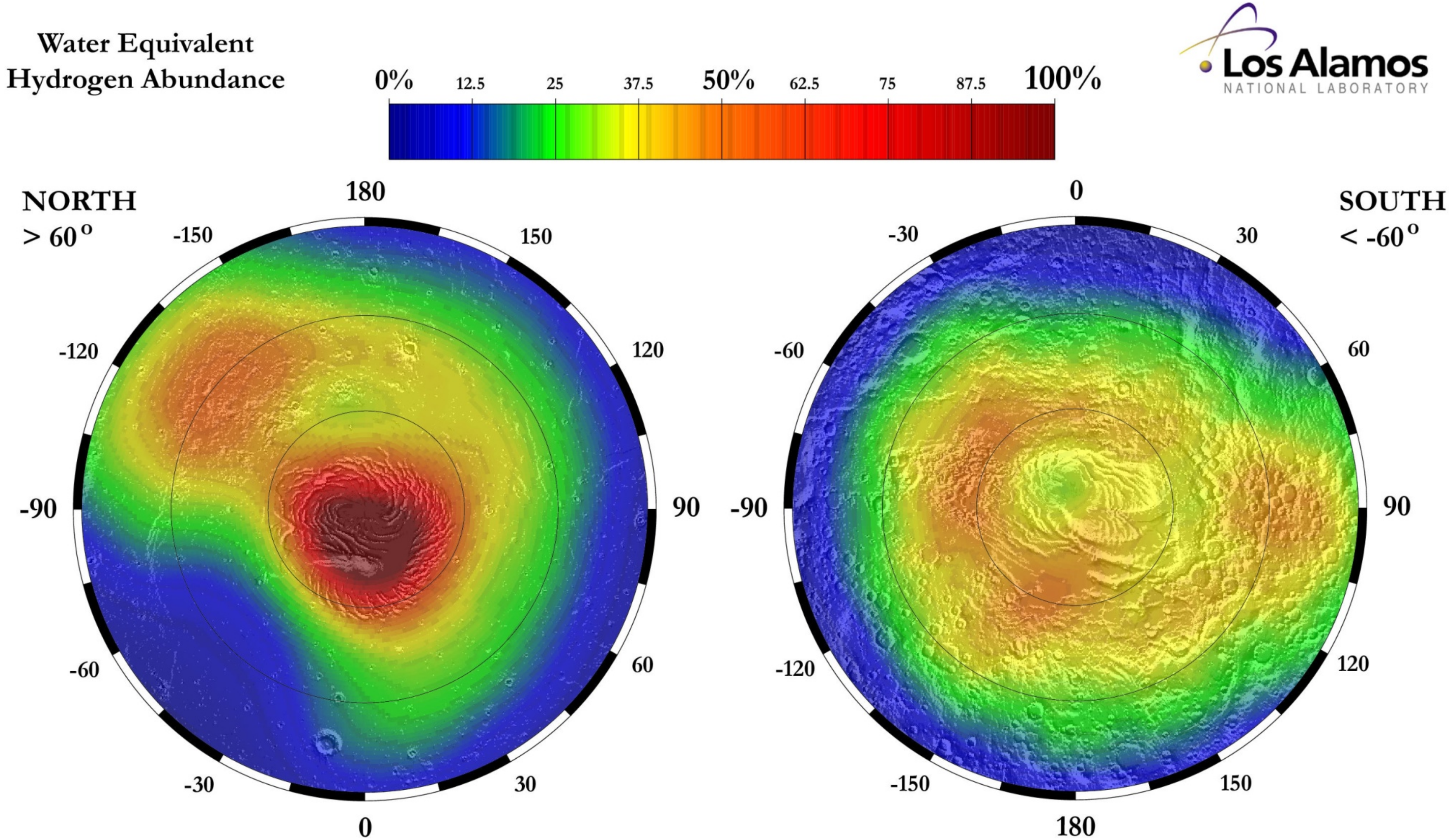

Distribution of Water on Mars: Overlay of water equivalent hydrogen abundances and a shaded relief map derived from MOLA topography. Mass percents of water were determined from epithermal neutron counting rates using the Neutron Spectrometer aboard Mars Odyssey between Feb. 2002 and Apr. 2003.

Reference: Feldman W. C., T. H. Prettyman, S. Maurice, J. J. Plaut, D. L. Bish, D. T. Vaniman, M. T. Mellon, A. E. Metzger, S. W. Squyres, S. Karunatillake, W. V. Boynton, R. C. Elphic, H. O. Funsten, D. J. Lawrence, and R. L. Tokar, The global distribution of near-surface hydrogen on Mars, *JGR-planets*, submitted July 2003.

These data were generated by the Planetary Science Team at Los Alamos: B. Barraclough, D. Bish, D. Delapp, R. Elphic, W. Feldman, H. Funsten, O. Gasnault*, D. Lawrence, S. Maurice*, G. McKinney, K. Moore, T. Prettyman, R. Tokar, D. Vaniman, and R. Wiens. * Also at Observatoire Midi-Pyrenees, France

The neutron spectrometer aboard Mars Odyssey, a component of the Gamma-ray Spectrometer suite of instruments, was designed and built by the Los Alamos National Laboratory and is operated by the University of Arizona in Tucson. The Mars Odyssey mission is managed by the Jet Propulsion Laboratory.

Mars Hydrogen from Neutron Measurements: Polar Regions

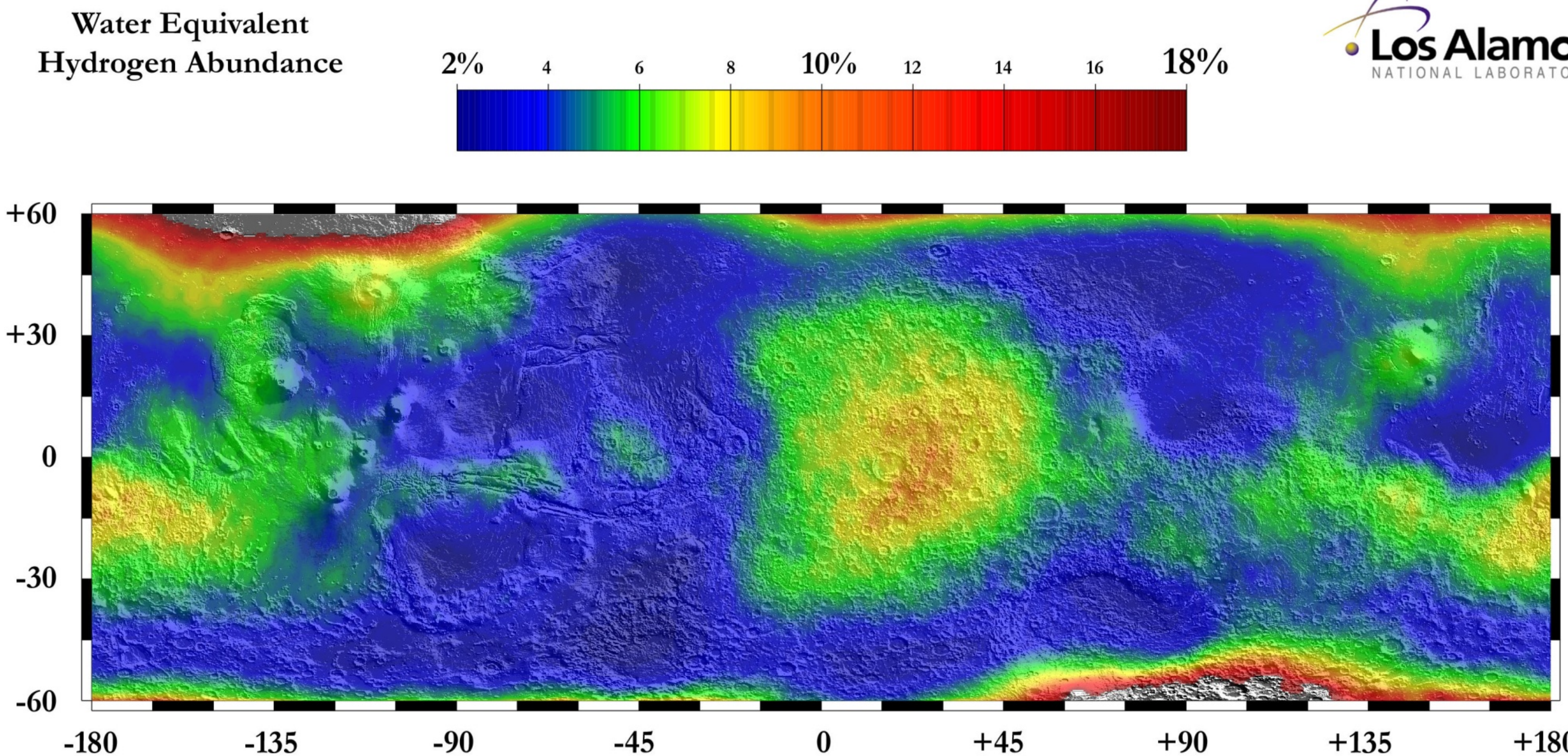

Los Alamos NATIONAL LABORATORY

Distribution of Water on Mars: Overlay of water equivalent hydrogen abundances and a shaded relief map derived from MOLA topography. Mass percents of water were determined from epithermal neutron counting rates using the Neutron Spectrometer aboard Mars Odyssey between Feb. 2002 and Apr. 2003.

Reference: Feldman W. C., T. H. Prettyman, S. Maurice, J. J. Plaut, D. L. Bish, D. T. Vaniman, M. T. Mellon, A. E. Metzger, S. W. Squyres, S. Karunatillake, W. V. Boynton, R. C. Elphic, H. O. Funsten, D. J. Lawrence, and R. L. Tokar, The global distribution of near-surface hydrogen on Mars, *JGR-planets*, submitted July 2003.

These data were generated by the Planetary Science Team at Los Alamos: B. Barraclough, D. Bish, D. Delapp, R. Elphic, W. Feldman, H. Funsten, O. Gasnault*, D. Lawrence, S. Maurice*, G. McKinney, K. Moore, T. Prettyman, R. Tokar, D. Vaniman, and R. Wiens. * Also at Observatoire Midi-Pyrenees, France

The neutron spectrometer aboard Mars Odyssey, a component of the Gamma-ray Spectrometer suite of instruments, was designed and built by the Los Alamos National Laboratory and is operated by the University of Arizona in Tucson. The Mars Odyssey mission is managed by the Jet Propulsion Laboratory.

Mars Hydrogen from Neutron Measurements: Mid and Low Latitudes

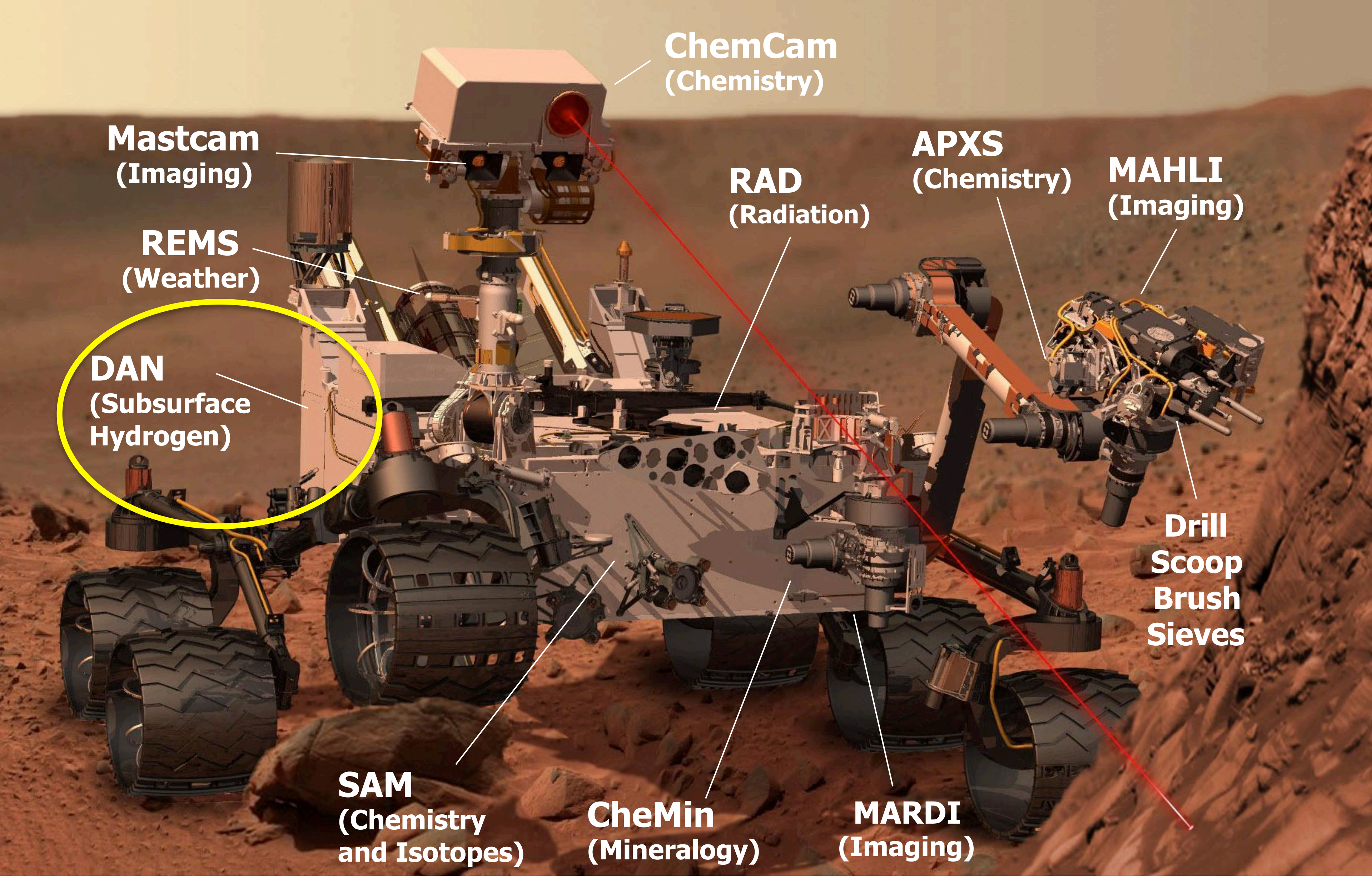
ChemCam
(Chemistry)
Mastcam
(Imaging)
RAD
(Radiation)
APXS
(Chemistry)
MAHLI
(Imaging)
REMS
(Weather)
DAN
(Subsurface
Hydrogen)
Drill
Scoop
Brush
Sieves
SAM
(Chemistry
and Isotopes)
CheMin
(Mineralogy)
MARDI
(Imaging)

CURIOSITY

Physics of DAN measurements:
Dynamic Albedo of Neutrons

No hydrogen in the soil

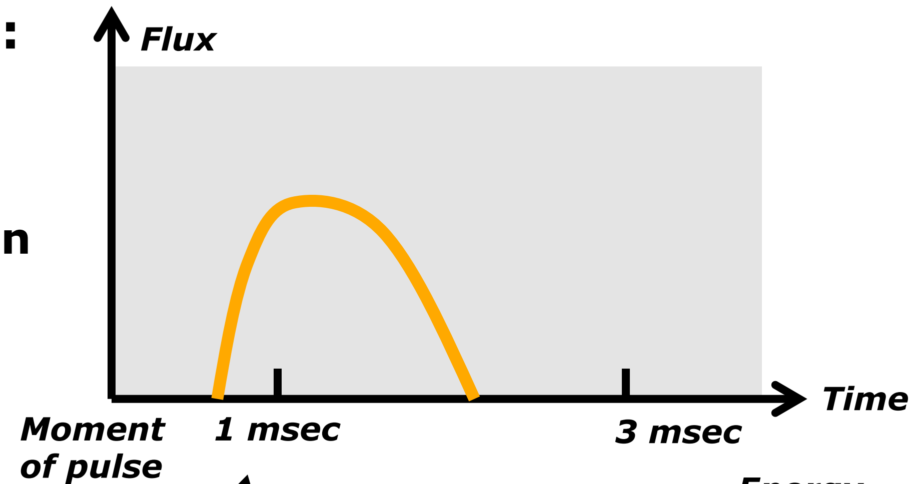

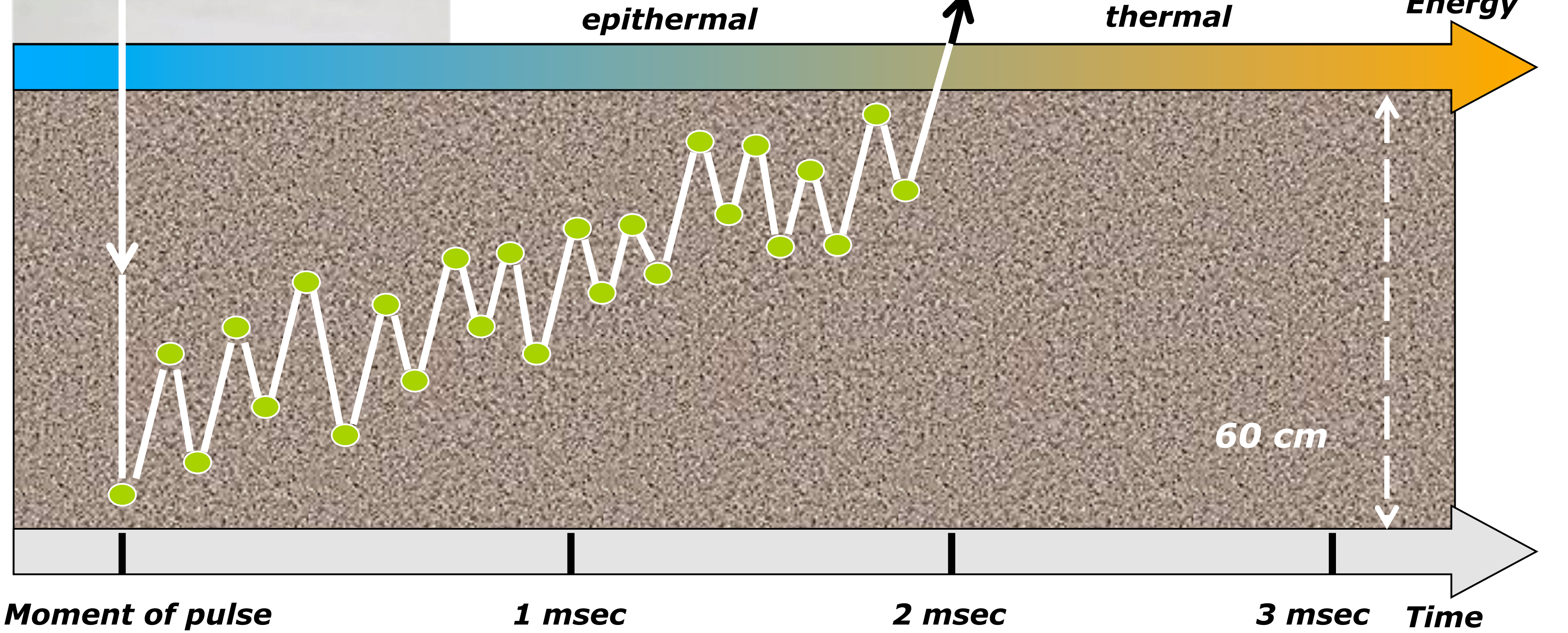

Physics of DAN measurements:
Dynamic Albedo of Neutrons

With hydrogen in the soil

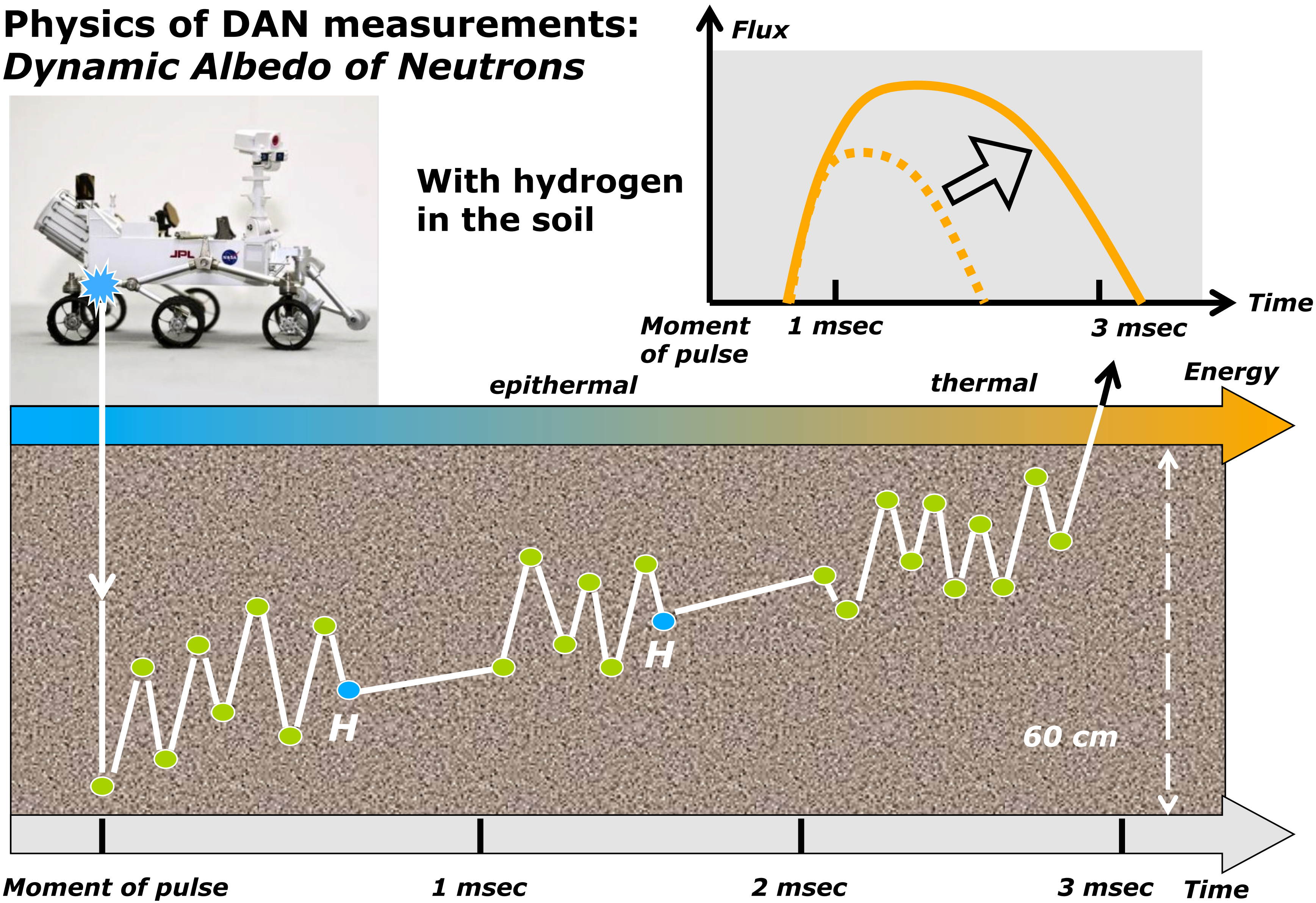

Variations of DAN data along the Curiosity traverse

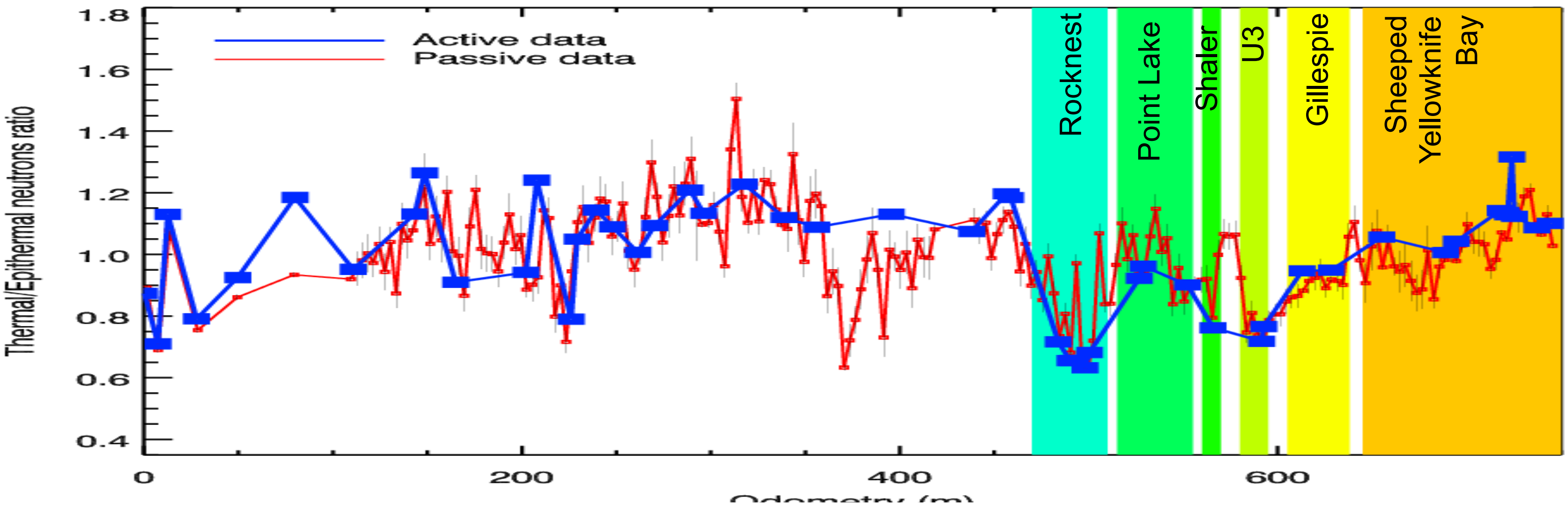

Variations of water content in the soil along the Curiosity traverse

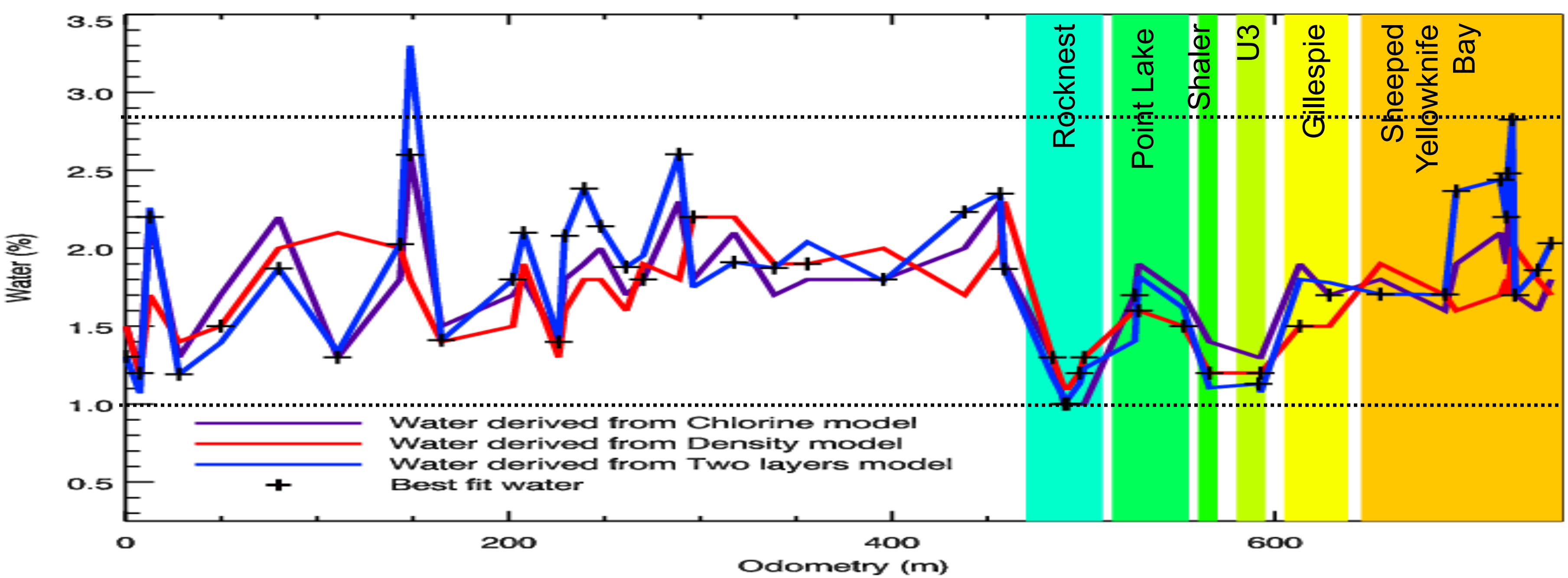

MSL in Yellowknife Bay

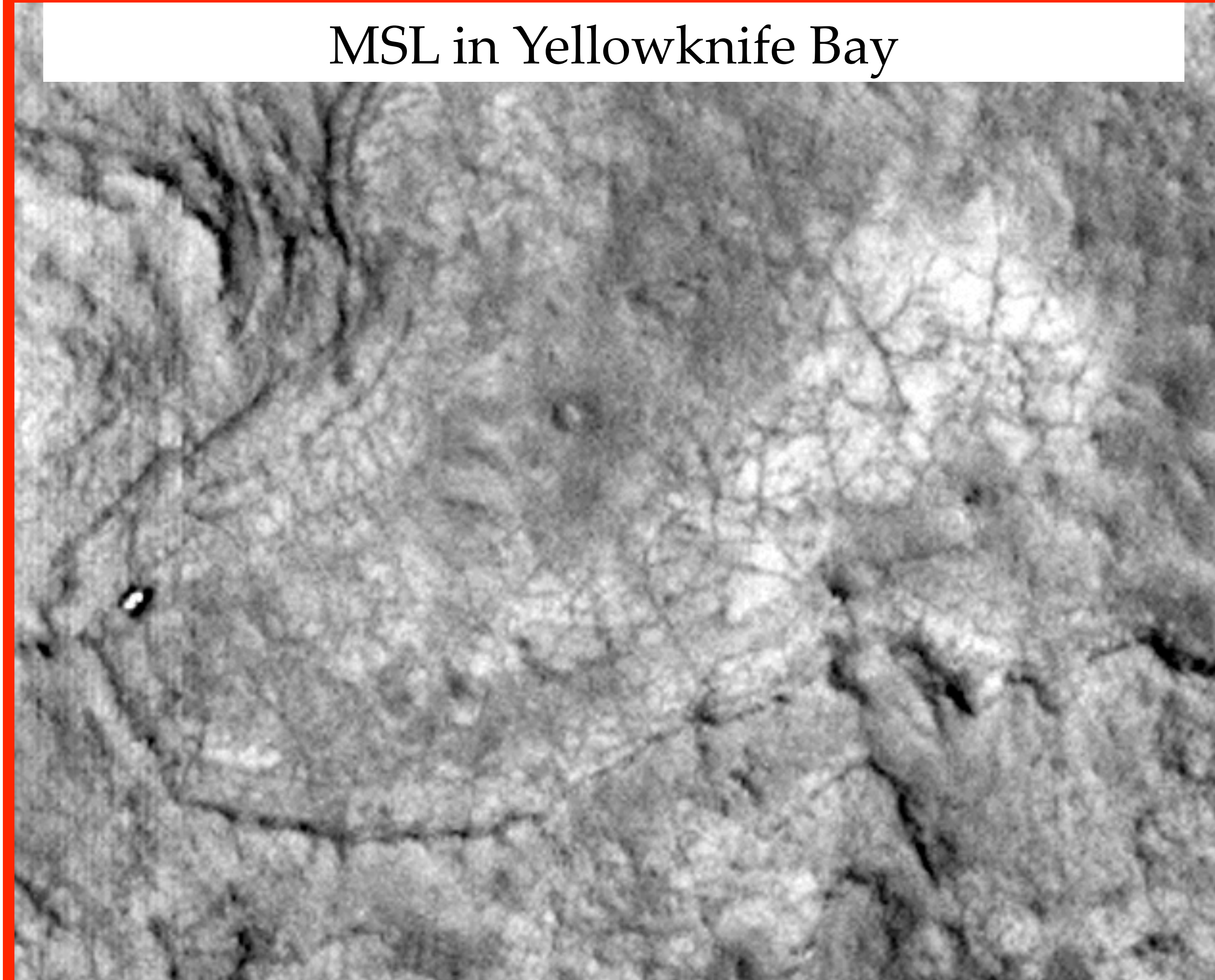

X-ray Fluorescence Spectroscopy

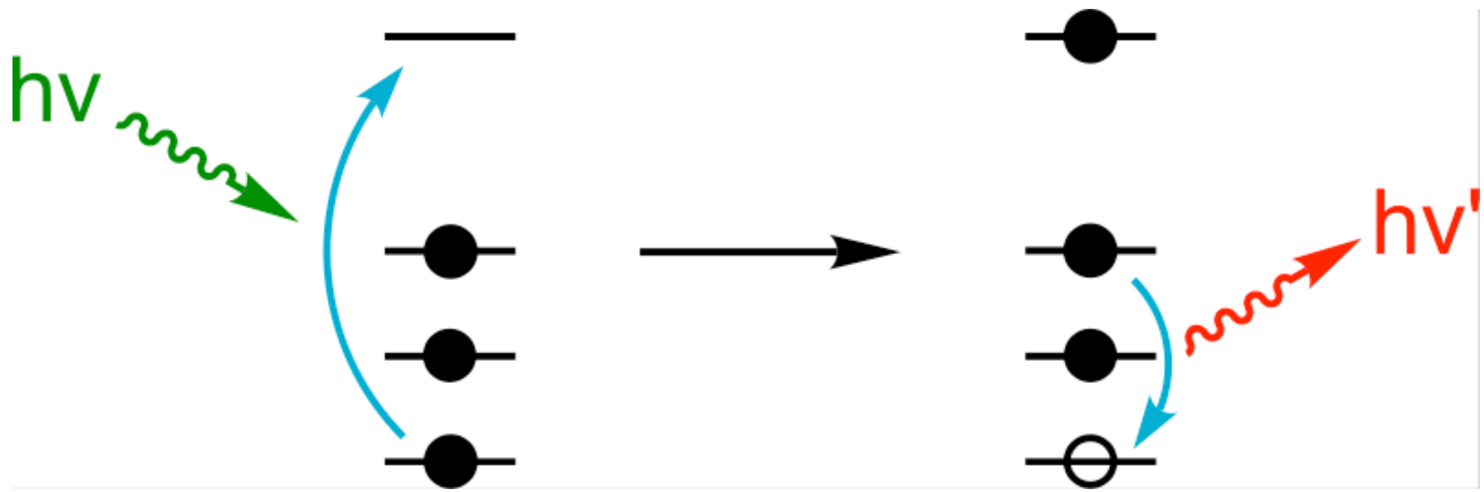

Particle and x-ray bombardment (from Sun, or a radioactive source) leads to ionization and subsequent electron cascade, causing fluorescence at wavelengths specific to each element

X-ray Fluorescence

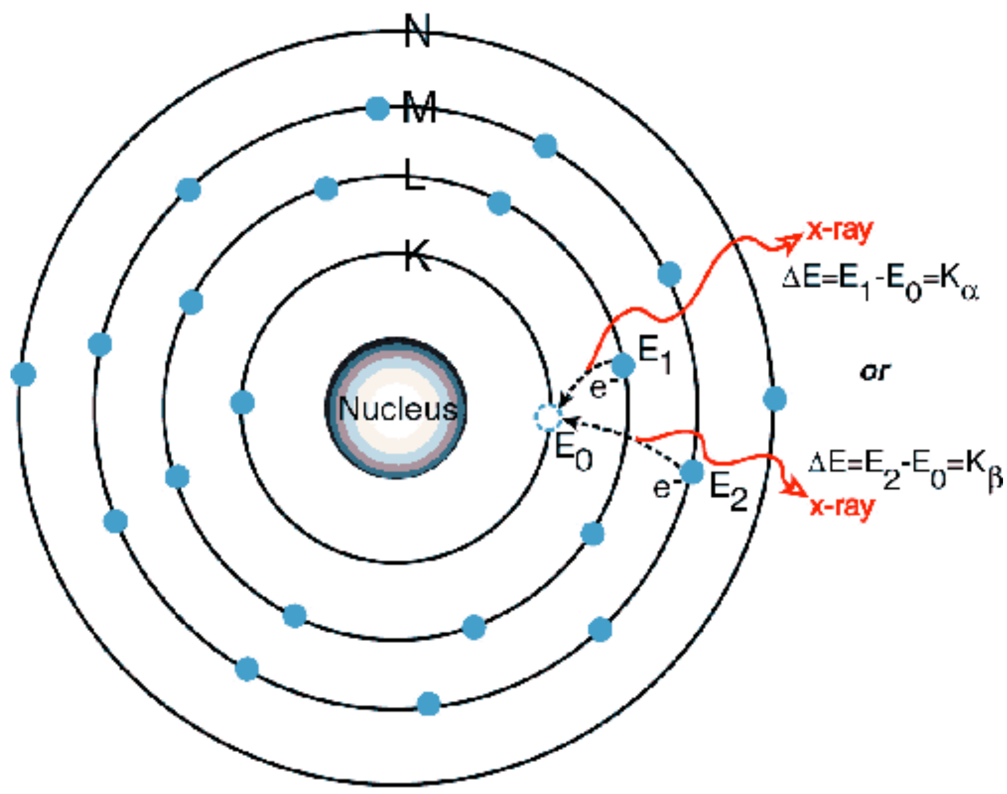

Particle and x-ray bombardment (from Sun, or a radioactive source) leads to ionization and subsequent electron cascade, causing fluorescence at wavelengths specific to each element

X-ray Fluorescence

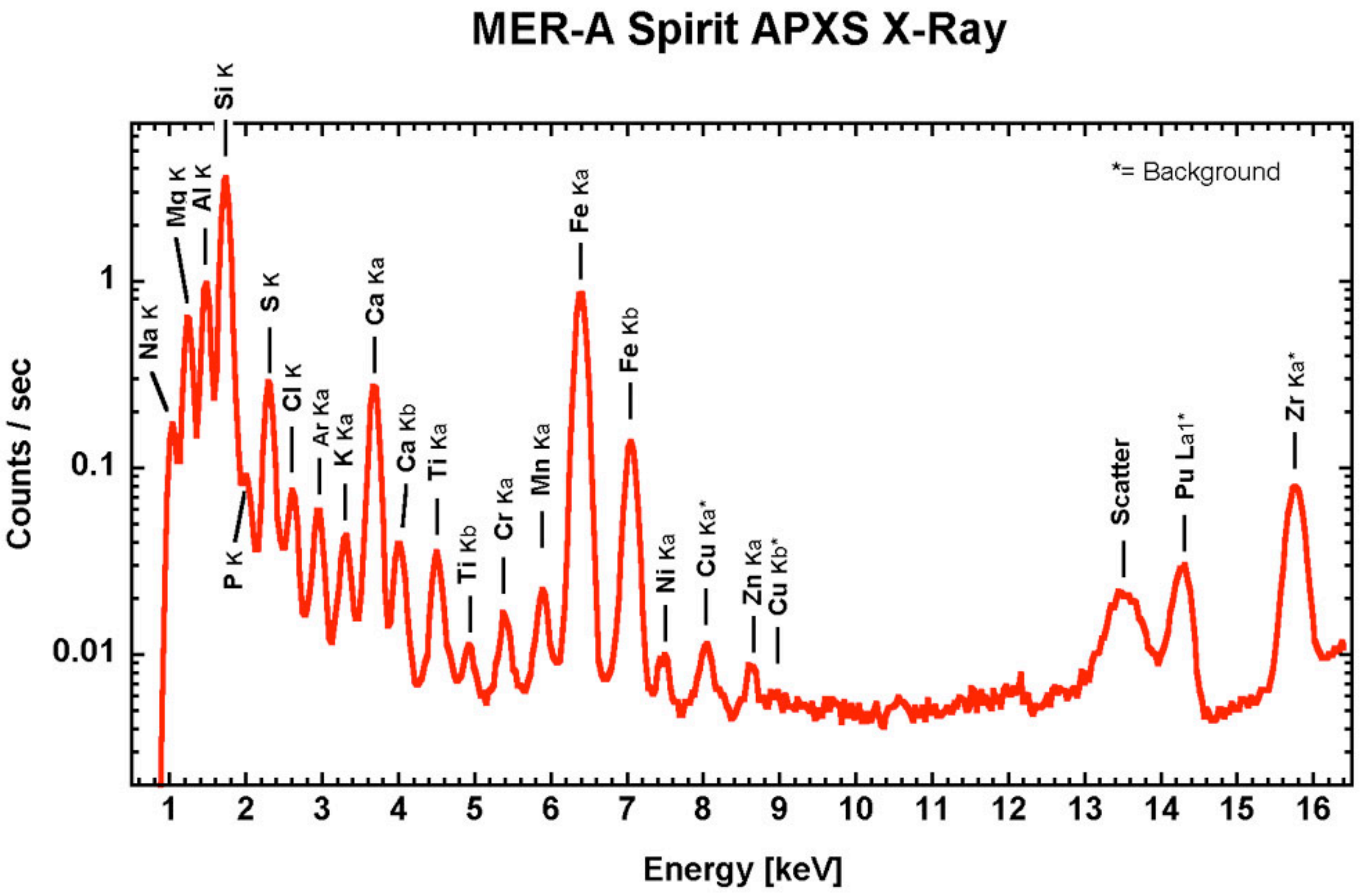

Similar instruments on Mars Pathfinder, Curiosity, Rosetta/Philae

For solar X-ray source, must monitor it simultaneously with your target

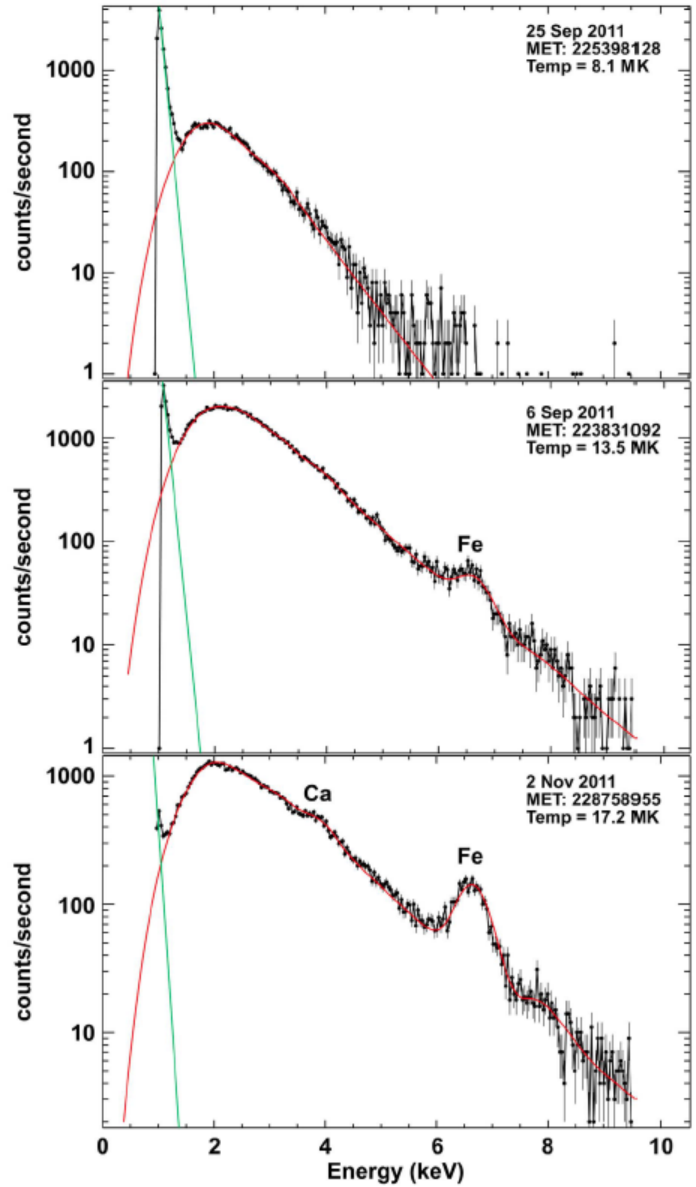

Figure 1. Three examples of fits to solar flare X-ray spectra measured by the SAX. The steeply inclined green line depicts the electronic background in the detector; the red line is the best fit solar spectrum (for the plasma temperature given in each case) convolved with the instrument response. The Ca and Fe line complexes (at ~3.6 keV and ~6.4 keV, respectively) increase in magnitude with temperature. MET = mission elapsed time, in s.

MESSENGER XRS
(at Mercury)

[Weider et al., 2012]

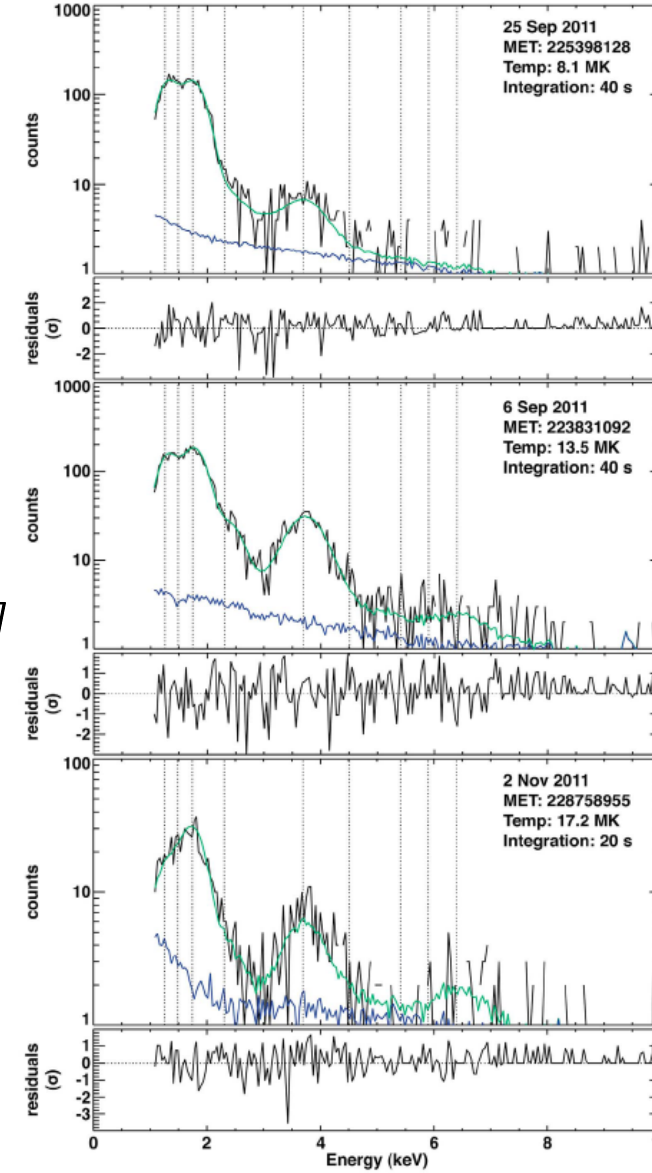

Figure 2. XRF spectra (black, primary signal) for the three time intervals for which solar spectra are shown in Figure 1. These spectra are the sum of the three separate GPC detector spectra. The best fit model (smooth curve) is shown in green, and the background level (lower signal) is shown in blue. Residuals between the best fit model and data are also shown in units of the counting-statistical error (σ) in each channel. Vertical dashed lines indicate the energy of K_α X-ray emission lines from (left to right) Mg, Al, Si, S, Ca, Ti, Cr, Mn, and Fe.

MESSENGER GRNS: Na heterogeneity

88 P.N. Peplowski et al./Icarus 228 (2014) 86–95

Table 1
Observed latitudinal variability of Na over the northern hemisphere of Mercury.

Latitude range	Average altitude (km)	Approximate spatial resolution[a] (km)	Na/Si abundance ratio	Na abundance (wt%)[b]
0–15°N	977	1500	0.115 ± 0.015	2.8 ± 0.4
15–30°N	646	1000	0.098 ± 0.016	2.4 ± 0.4
30–45°N	447	700	0.123 ± 0.019	3.0 ± 0.4
45–60°N	343	500	0.103 ± 0.018	2.5 ± 0.4
60–75°N	351	500	0.129 ± 0.019	3.2 ± 0.4
75–90°N	456	700	0.172 ± 0.020	4.2 ± 0.5
0–60°N			0.107 ± 0.008	2.6 ± 0.2
80–90°N			0.198 ± 0.030	4.9 ± 0.7

[a] The spatial resolution for an omnidirectional Gamma-Ray Spectrometer is approximated as 1.5 times the orbital altitude.
[b] Na abundance is calculated under the assumption of a constant Si abundance of 25 wt% across the surface (see Evans et al., 2012).

High Na abundances around Mercury's north polar region ➔ alkali feldspar-rich volcanic plains?